Annu. Rev. Earth Planet. Sci. 1992. 20:553–600

SILICATE PEROVSKITE

Russell J. Hemley and Ronald E. Cohen

Geophysical Laboratory and Center for High Pressure Research,
Carnegie Institution of Washington, Washington, DC 20015

KEY WORDS: mineralogy, Earth's lower mantle, high pressure, ferromagnesian silicate, calcium silicate, physical properties of minerals

INTRODUCTION

High-pressure experiments have established that the silicate minerals that comprise the Earth's crust and upper mantle transform to assemblages dominated by minerals having perovskite-type structures at pressures corresponding to those of the lower mantle. This region of the Earth's interior extends from 670 km to 2900 km depth and occupies approximately 60% of the volume of the planet. The observation of the high-pressure stability of silicate perovskite has opened up the possibility of understanding the mineralogy of this vast region of the planet's interior. Indeed, characterization of the chemical and physical properties of a range of silicate perovskites during the past fifteen years has provided new constraints on the composition and structure of the mantle, new insights into core-mantle interaction and coupling, and new bounds on mantle and core formation and long-term evolution.

Significant progress in understanding the properties of silicate perovskites has been made in the past five years. A number of obstacles have been encountered in the study of these high-pressure phases, owing to both the small quantities in which they can be synthesized in the laboratory and their intrinsic instability at low (e.g. ambient) pressure conditions. The recent progress in investigations of silicate perovskites has been made possible in large measure by advances in high-pressure techniques, such as diamond-cell methods including synchrotron radiation and laser techniques, multi-anvil press technology which has made possible the preparation of single crystals and petrologic studies, and advances in theoretical calculations such as new accurate electronic-structure methods. As a result

0084–6597/92/0515–0553$02.00

of these advances, the implications for the Earth on a global scale—many of which were speculations based on, at best, educated guesses just a few years ago—are now grounded on experimental data supported by a growing theoretical understanding. The emerging body of data on these materials also provides a firm basis for ruling out alternative models. On the other hand, a number of outstanding issues remain, and these have given rise to some recent controversies regarding the properties of perovskite and their geophysical implications.

Several reviews of various aspects of silicate perovskites and our current understanding of their implications for the Earth and planetary interiors have appeared during the last few years (Liu & Bassett 1986, Navrotsky & Weidner 1989, Hazen 1988, Anderson 1989). In this paper we review the mineralogy and properties of this class of geophysically and geochemically important materials, emphasizing recent experimental data, theoretical insights, and current problems. This is a field of active research, and we present this review as a progress report rather than as review of a settled subject. In the next few years, we expect many of the issues raised here to be solved by further experiments under P-T conditions of the lower mantle and by development and application of refined theoretical methods.

CRYSTAL CHEMISTRY

The perovskite structure for a stoichiometric compound with a composition ABX_3 consists of corner sharing anion X octahedra containing B cations with larger A cations between the octahedra. In the perovskite-type silicates, tetravalent silicon occupies the smaller B site, with a variety of other (typically divalent) cations (Mg, Fe, Ca) in the A site. The ideal, high symmetry structure (aristotype) is shown in Figure 1*a*. A variety of distortions from this ideal structure are possible in general (Glazer 1972, 1975; Aleksandrov 1976, 1978; Salje 1989). These include various combinations of coupled rotations and cation displacements (off-centering). Some octahedral-tilting transitions can be understood in terms of condensation of phonons at the boundary of the Brillouin zone, and other transitions are by necessity first-order phase transitions (see below). Glazer (1972) discussed the classification of distorted perovskites that involve nearly rigid rotations of the oxygen octahedra. In Glazer's notation, the tilts in the *Pbnm* structure are of type ($a^-a^-c^+$), which means that the octahedra are tilted along an axis parallel to c with the same direction of tilts in adjacent planes along c (c^+), and are tilted by a different rotation angle along a and b with opposite directions of tilts in adjacent planes (Figure 1*b*). Aleksandrov (1976, 1978) used a different notation which emphasizes the relationship of the c^+ type tilt to an M-point phonon

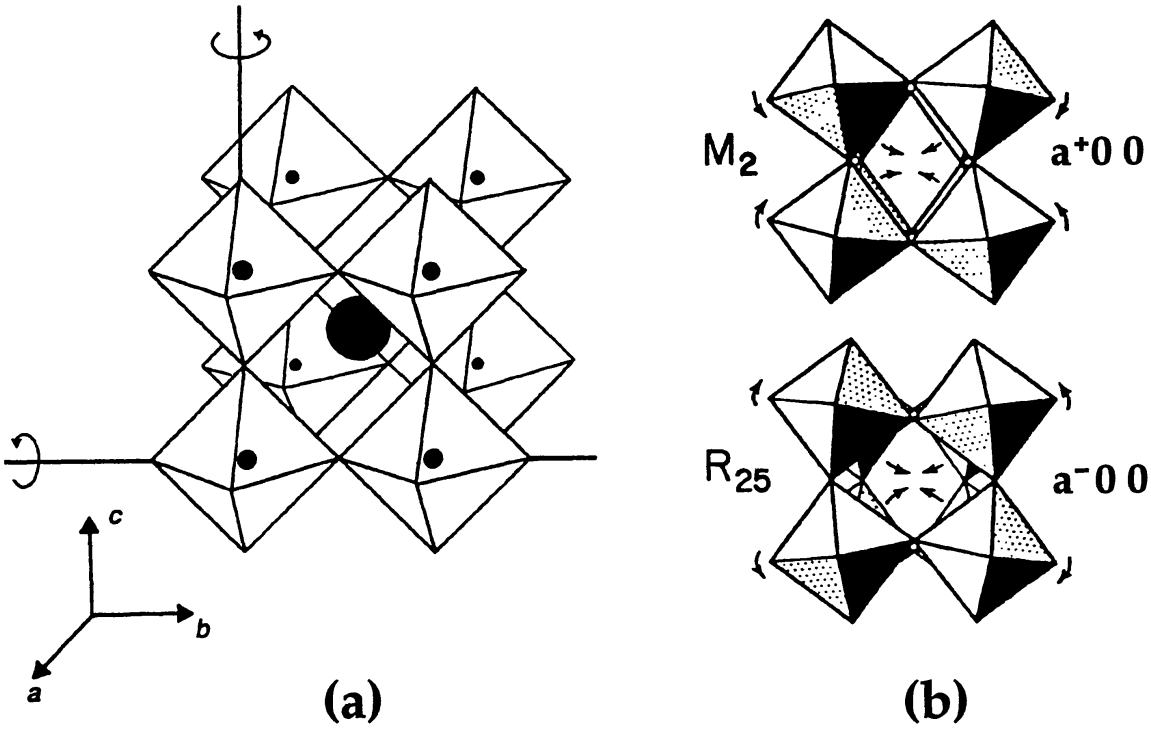

Figure 1 (*a*) Ideal perovskite structure for ABX_3 compounds, illustrating the corner-shared BX_6 octahedra. Two rotation axes leading to tilts are shown with the arrows. (*b*) Combinations of tilts giving rise to the *R*- and *M*-point instabilities (modified from Wolf & Jeanloz 1985).

instability and the a^- type tilts to an *R*-point instability, as discussed below.

The structure of $(Mg,Fe)SiO_3$ perovskite (over the *P-T* range under which it has been studied experimentally) is orthorhombic, with space group *Pbnm*. This structure was proposed on the basis of powder x-ray diffraction on $MgSiO_3$ by Yagi et al (1977, 1978a) and Ito & Matsui (1978), who studied the material quenched to room conditions. This structure was confirmed by single crystal x-ray diffraction techniques by Horiuchi et al (1987). A significant recent advance is the development of techniques for growth of single crystals (Ito & Weidner 1986) for x-ray structure determination and other techniques requiring high-quality single crystals (see below). The single-crystal structure of Horiuchi et al (1987) is very close to that proposed by Yagi et al (1977, 1978a) and Ito & Matsui (1978). The larger, pseudo-tetragonal unit cell suggested by early transmission electron microscopy and diffraction measurements (Madon et al 1980) has been reinterpreted in terms of a high degree of twinning of crystals with the *Pbnm* orthorhombic structure (Madon et al 1989).

In $MgSiO_3$ the tilt angle around c is 11.2°, and the angle of tilt around a and b is about 16.7°. The unit cell in $MgSiO_3$ is rotated approximately 45° from that in cubic perovskite with the new a- and b-axes approximately equal to $\sqrt{2}a'$, where a' is the cubic lattice parameter, and the c-axis is doubled. Thus the unit cell size is quadrupled with 20 atoms in the primitive unit cell. The orthorhombic $MgSiO_3$ perovskite has the axial ratio $a:b:c = 0.968:1:1.394$, which differs from the equivalent ratio of the ideal cubic perovskite, 1:1:1.414. In contrast, $CaSiO_3$ crystallizes in the high-symmetry cubic perovskite structure at high pressure (Liu & Ringwood 1975). This difference in the structures of $(Mg,Fe)SiO_3$ and $CaSiO_3$ is due to the small size of the ion in the A site relative to that in the B site. The effects of the ratio of the cation ionic radii on the structure have been examined in detail in perovskites that may be considered analogues to silicate perovskites (Sasaki et al 1983). This relationship is generally supported by theoretical calculations based on the ionic model (Hemley et al 1985, 1987; Wolf & Jeanloz 1985; Wolf & Bukowinski 1985, 1987). These calculations predict that the cubic $CaSiO_3$ should transform to the lower symmetry orthorhombic perovskite structure at high compressions, although this has not yet been observed experimentally. Thus, despite the variety of structures observed in perovskites (e.g. Glazer 1972), only two structure-types (cubic *Pm3m* and orthorhombic *Pbnm*) appear to be mineralogically significant for lower mantle silicates. Others have been predicted theoretically and are likely to occur on crystal chemical grounds for other compositions (see below).

Iron enters the orthorhombic $MgSiO_3$ perovskite up to a mole fraction of ~20% (see below). The effect on the molar volume is shown in Figure 2, which summarizes early powder diffraction results and the results of more recent crystal structure refinements by the Reitveld powder method (Parise et al 1990) and single-crystal techniques (Kudoh et al 1990) using synchrotron radiation. Iron substitution affects the structure by causing a decrease in the degree of distortion. Aluminum is also soluble in the orthorhombic perovskite, with a maximum solubility of 25% (Weng et al 1982), and results in a significantly larger increase in the unit-cell volume. Although substitution of both Fe and Al expands the structure, the former results in a decrease in distortion from cubic (smaller octahedral tilts) whereas the latter causes the distortion to increase. Weng et al (1982) propose that the increase in distortion on addition of Al arises from equal distribution of the trivalent cation on both the A and B sites [i.e. $(Mg,Al)(Si,Al)O_3$], which results in inefficient packing. Preliminary evidence for the effect of simultaneous Fe and Al substitution has been reported recently (O'Neill et al 1991).

The coordination of iron and cation site occupancy in $(Mg,Fe)SiO_3$

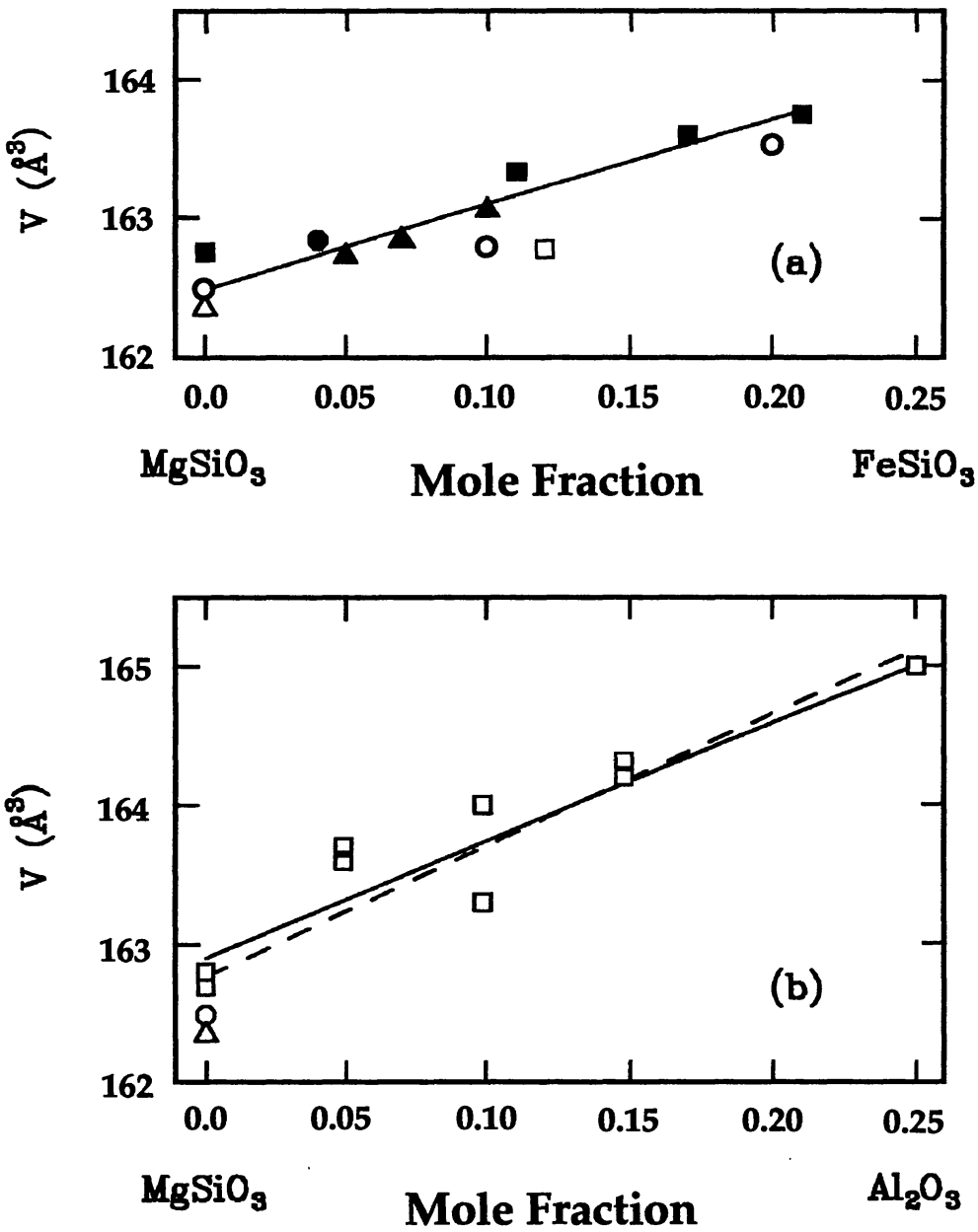

Figure 2 (*a*) Unit-cell volume of the Mg-rich orthorhombic perovskite as a function of mole fraction of $FeSiO_3$ component. ■, Yagi et al (1978b); △, Ito & Matsui (1978); ▲, Ito & Yamada (1982); □, Knittle & Jeanloz (1987a); ●, Kudoh et al (1990); ○, Mao et al (1991). The solid line is the fit $V(Å^3) = 162.48(7) + 6.2(7)X_{Fe}$ reported by Kudoh et al (1990). (*b*) Unit-cell volume as a function of mole fraction of Al_2O_3. □, Weng et al (1982); △, Ito & Matsui (1978); ○, Mao et al (1991). The solid line is the fit $V(Å^3) = 162.9 + 8.4X_{Al}$ reported by Weng et al (1982). The dashed line is a fit that includes the more recent zero-pressure data: $V(Å^3) = 162.9(1) + 9.4(9)X_{Al}$.

perovskite has been the subject of much recent discussion. On the basis of EXAFS (extended x-ray absorption fine structure) measurements on $(Mg,Fe)SiO_3$ samples synthesized in a diamond-cell, Jackson et al (1987) propose that Fe substitutes for Si, with an associated vacancy and occupation of the 12-fold A site by Si. Evidence for two different Fe sites from Mössbauer measurements of diamond-cell samples of $(Mg,Fe)SiO_3$ perovskite was interpreted in terms of mixing of Fe on the A and B sites (K. Weng et al, unpublished). In addition to its crystal chemical significance, such behavior would give rise to an important entropic stabilization of perovskite and perhaps unusual geochemical properties at high temperatures. More recent measurements have been interpreted as evidence for Fe occupying the A site alone (Jeanloz et al 1991). On the other hand, the single-crystal x-ray diffraction data of Kudoh et al (1990) and powder x-ray diffraction and XANES (x-ray absorption near-edge spectroscopy) measurements of Parise et al (1990) on perovskite samples synthesized in multi-anvil devices show no evidence for anomalous site occupancy. Recent NMR measurements on ^{29}Si-enriched $MgSiO_3$ perovskite, also synthesized in a multi-anvil device, indicate highly ordered Si in octahedral coordination with no Si in the A site (Kirkpatrick et al 1991). Unfortunately, similar tests on iron-bearing samples are not possible because Fe forms paramagnetic impurities which overwhelm the NMR signal. Differences in samples resulting from differing preparation procedures—including P-T range, approach to equilibrium, impurities, fO_2, point defects, and Fe^{+3} content—could be responsible (Hirsch & Shankland 1991). The observation of octahedral Fe in such samples would be expected if a small amount of glass or magnesiowüstite is present (see below), since Fe partitions into melt and the oxide relative to perovskite (Bell et al 1979, Heinz & Jeanloz 1987). Although there is now good agreement on many of the measured physical properties of perovskite, differences in the behavior of samples synthesized in diamond-cell and multi-anvil devices are evident and not fully understood.

Knowledge of the effects of pressure and temperature on the crystal structure is essential for understanding the properties of the material under mantle conditions. This includes possible displacive transitions, which may give rise to anomalous changes in physical properties with important consequences for the interpretation of geophysical data (see below). Pressure effects on the structure of Mg-rich silicate perovskites have been determined under hydrostatic conditions by both single-crystal and powder x-ray diffraction (Yagi et al 1982; Kudoh et al 1987; Ross & Hazen 1989; Mao et al 1989b, 1991). Figure 3 summarizes the effects of P and T on the axial (lattice-parameter) ratios c/a and b/a for $(Mg,Fe)SiO_3$ perovskites. The experimental data show that the orthorhombic

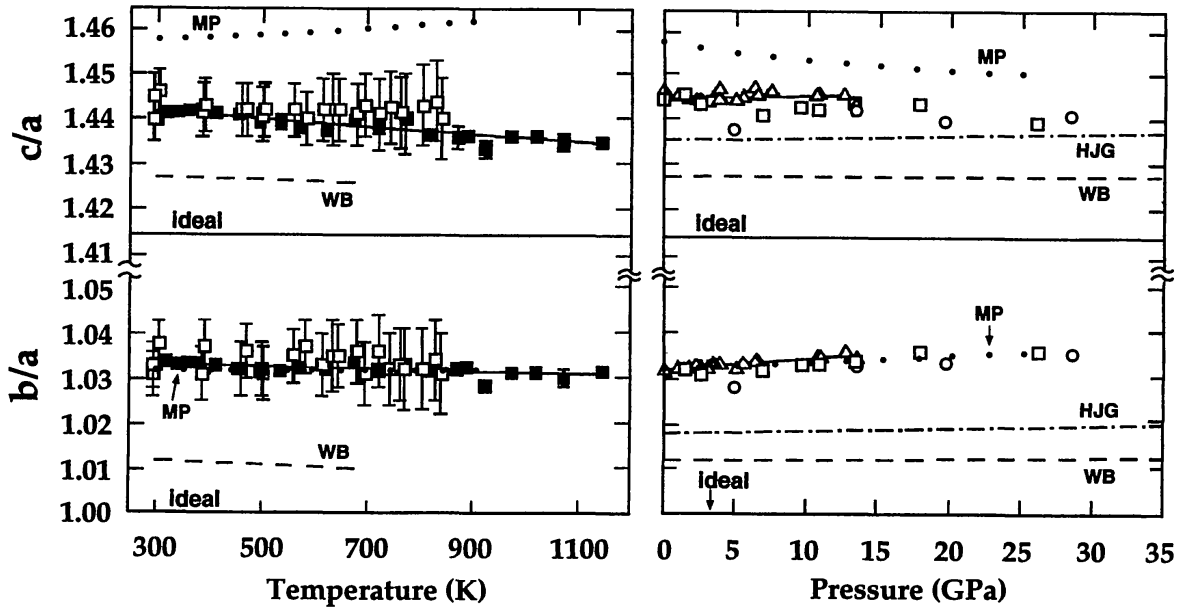

Figure 3 Effect of pressure and temperature on the unit-cell axial ratios for orthorhombic $(Mg,Fe)SiO_3$. Experimental high-temperature ($\gtrsim 300$ K) are included: □, Knittle et al (1986); ■, Wang et al (1991a). The high-pressure data are hydrostatic results: △, Ross & Hazen (1990); ○, □, Mao et al (1991). The predictions of nonempirical theoretical ionic model calculations are shown by the dot-dashed line (*HJG*—Hemley et al 1987) and the dashed line (*WB*—Wolf & Bukowinski 1987). The dotted line is the result of the molecular dynamics simulation using potentials fit to experimental data (*MP*—Matsui & Price 1991, and to be published).

$(Mg,Fe)SiO_3$ perovskite is elastically anisotropic with the *b*-axis having the smallest linear compressibility, β_b, approximately 25% smaller than β_a or β_c (Table 1). The *a* and *c* compressibilities are similar, with *c* slightly more compressible. With increasing pressure, the difference between *a* and *b* increases and the structure becomes more distorted, consistent with crystal chemical arguments (O'Keeffe et al 1979) and theoretical calculations (Hemley et al 1987), although the changes are relatively small. These changes also indicate that the material becomes more elastically anisotropic with pressure (Meade & Jeanloz 1991). The temperature changes are also relatively small over the range of existing measurements, and the axial ratios remain far from their ideal values (Knittle et al 1986, Ross & Hazen 1989, Parise et al 1990). Nevertheless, recent measurements to ~ 1200 K do show a decrease in *c*/*a* and *b*/*a* (Wang et al 1991a). The temperature effects largely mirror the pressure effects over the range of the measurements, suggesting that the structural changes are largely controlled by volumetric terms (e.g. Hemley et al 1987). Perovskites containing open-shell cations may not exhibit the same *P-T* effects on structure because of the higher degree of directional bonding (crystal-field effects) in such compounds (e.g. $SrZrO_3$, Andrault & Poirier 1991).

Table 1 Zero-pressure bulk modulus and linear compressibilities of $(Mg_{1-x}Fe_x)SiO_3$ perovskite (298 K)

K_0 GPa	K_0'	β_{a0} TPa^{-1}	β_{b0} TPa^{-1}	β_{c0} TPa^{-1}	P_{max} GPa	P media[a]	Sample[b]	x	Reference[c]
246	---	1.31	1.20	1.56	0	---	SC	0	Yeganeh-Haeri et al (1989a,b)
247	4	1.41	1.07	1.57	10	M-E-W	SC	0	Kudoh et al (1987)
254	4	1.30	1.04	1.24	13	M-E, Ne	SC	0	Ross and Hazen (1989)
258	4	1.58	1.19	1.10	7	M-E	P	0	Yagi et al (1982)
266	3.9	---	---	---	112	none	P	0.12	Knittle and Jeanloz (1987a)
261	4	1.34	1.08	1.43	30	Ne	P	0, 0.1, 0.2	Mao et al (1991)
---	---	1.29	1.03	1.31	7	NaCl	P	0	Wang et al (1991a)

[a] M-E: methanol-ethanol mixture; M-E-W: methanol-ethanol-water mixture.
[b] SC: single crystal; P: powder.
[c] Adiabatic bulk modulus and compressibilities were measured using Brillouin scattering at zero pressure by Yeganeh-Haeri et al (1989a,b). Isothermal moduli and compressibilities were determined from fitting *P-V-a-b-c* data measured by x-ray diffraction techniques in the remaining studies.

BONDING AND ENERGETICS

Considerable insight into the crystal chemistry, bonding, and basis of physical properties has been obtained from calculations using theoretical and computational methods. Calculations with nonempirical theoretical models based on first principle methods have been particularly useful. These calculations correctly predict the *M*- and *R*-point instabilities that lead to the *Pbnm* structure for $MgSiO_3$ (Hemley et al 1985, 1987; Wolf & Jeanloz 1985; Wolf & Bukowinski 1987). One of the goals of these techniques is an accurate prediction of the density, equation of state, and structural properties of the crystal from a single, unified model. Several sets of calculations based on the Gordon-Kim (electron-gas) model have been performed. Hemley et al (1985, 1987) used a modified electron-gas approach to examine principally the structural distortions at zero pressure and at high compression. Wolf & Jeanloz (1985) and Wolf & Bukowinski (1987) applied an earlier version of the electron-gas model and found good agreement for the bulk modulus. Cohen (1987) used the potential induced breathing (PIB) model, which includes dynamical charge relaxation effects and different assumptions within the Gordon-Kim approximation; good agreement was obtained for the bulk modulus and predictions for the single crystal elastic moduli were made. A variety of calculations based on empirical potentials have also been performed (e.g. Miyamoto & Takeda 1984, Wall et al 1986, Matsui et al 1987, Matsui 1988, Price et al 1989, Wright & Price 1989, Reynard & Price 1990, Matsui & Price 1991). These calculations have been useful for predictions of structural properties, defect

energies, and high P-T behavior (see below). One important detail that is very difficult to describe accurately with various potential models is the exact degree of distortion from the cubic structure and its variation with pressure. This is because the distortion depends critically on a delicate interplay between the Si-O and Mg-O interactions, as well as the O-O interaction.

All of the above calculations assumed an ionic description of the bonding in silicate perovskite and their general qualitative success indicates that $MgSiO_3$ is likely to be very ionic in comparison to lower pressure silicate minerals having tetrahedrally coordinated Si. Electronic structure calculations on cubic $MgSiO_3$ perovskite have been performed to determine the degree of covalent relative to ionic bonding and to obtain the electronic band structure (Cohen et al 1989) (Figures 4 and 5). These calculations, which appear to represent the best description to date of the bonding in silicate perovskites, show that the Mg is nearly a perfectly spherical Mg^{2+} ion. There is some charge transfer back to Si from O and the charges are less than the nominal Si^{4+} and O^{2-}. The valence charge on Si has both s and d character. There is also a small covalent bond charge in between the Si and O that contains about 0.1 electrons. Although $MgSiO_3$ is very ionic, it is not described particularly well by a rigid ion model. In fact, the oxygen ion density changes with pressure. If this "breathing" of the oxygen ions is not included, it is difficult to describe accurately both the elastic properties and the equation of state (pressure-volume relations).

Three relatively strong predictions of theoretical calculations are that

1. The distortion (tilts) should increase with pressure, and the energy difference between the equilibrium distorted structure and the undistorted cubic structure increases with pressure;
2. the distorted phase is significantly denser than the undistorted structure at a given pressure; and
3. the cubic structure has a higher bulk modulus than the orthorhombic structure.

The effect of Fe substitution, which is expected to lower the band gap and introduce crystal field stabilization and additional directional bonding, has not yet been explored in these calculations. Theoretical calculations on other iron-bearing oxides, simplified models, and available experimental data suggest that small amounts of Fe soluble in silicate perovskite do not greatly affect its cohesive and elastic properties (e.g. Wright & Price 1989). On the other hand, as discussed below, Fe significantly affects the electrical conductivity and other transport properties, as might be expected from its open-shell character.

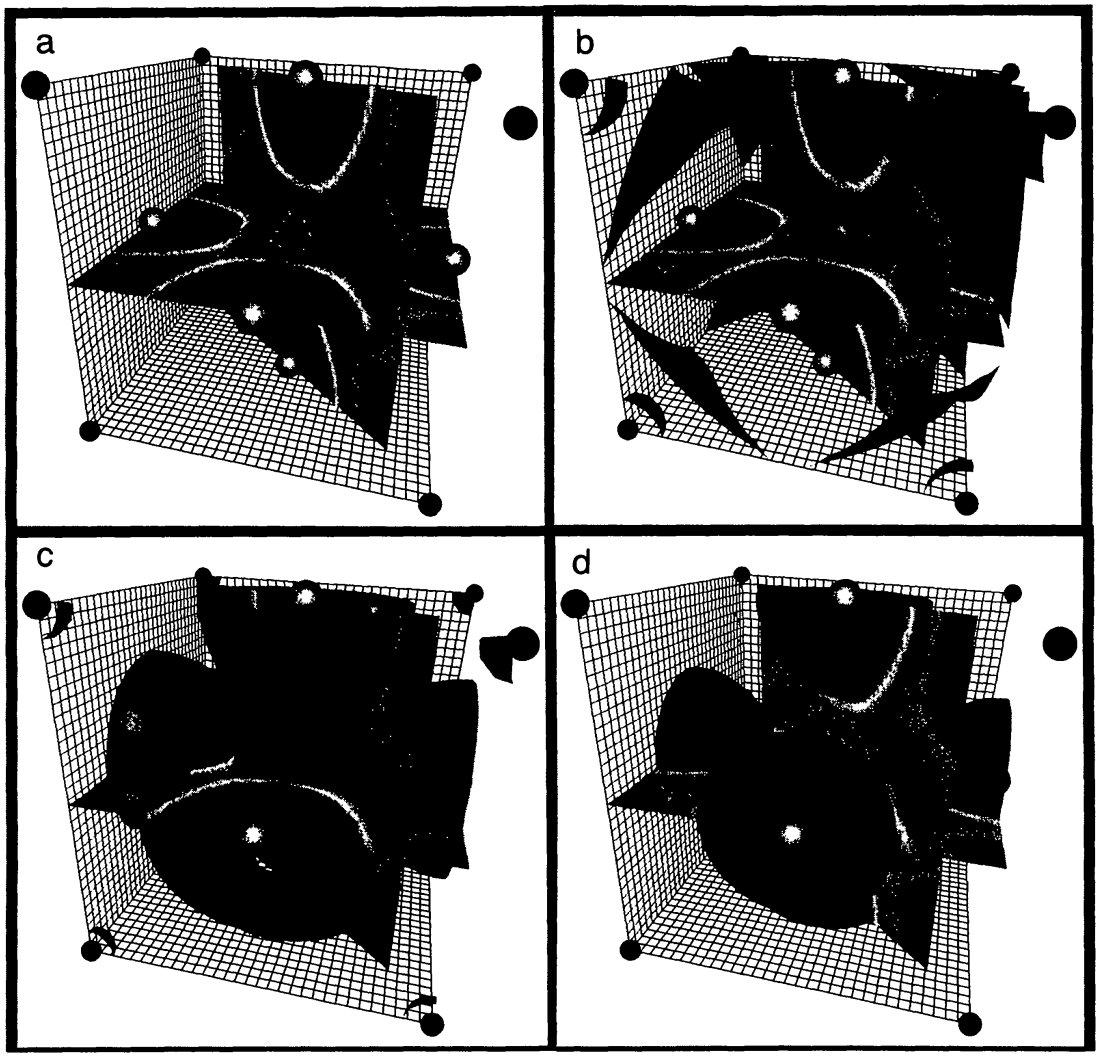

Figure 4 Calculated valence charge density for cubic $MgSiO_3$ perovskite using the LAPW method. The valence charge density is the electron density associated with chemical bonding. In $MgSiO_3$ perovskite the valence charge density is very ionic (i.e. mostly O^{2-}) but there is some hybridization with the Si *d* and *s* states. (*a*) Two slice planes along (*001*) and (*110*). The magnesium ions are at the corners, the oxygen ions are at the centers of the faces, and silicon is at the center. (*b*) Low-density isosurface at a density of 0.014 electrons (e^-)/bohr^3 (1 bohr = 0.529 Å). Note the density around the Mg ions at the corners and the interesting cubic box of density around the Si at the center. (*c*) Isosurface at 0.05 e^-/bohr^3. This surface indicates there is excess charge in the triangles formed between two oxygens and the Si, as illustrated by the "necking" of the surfaces. (*d*) Contour level of 0.1 e^-/bohr^3. The principal contribution to the higher density surfaces is from the oxygen, though there is also a small region of spherical charge around the Si, which consists primarily of Si *s* states.

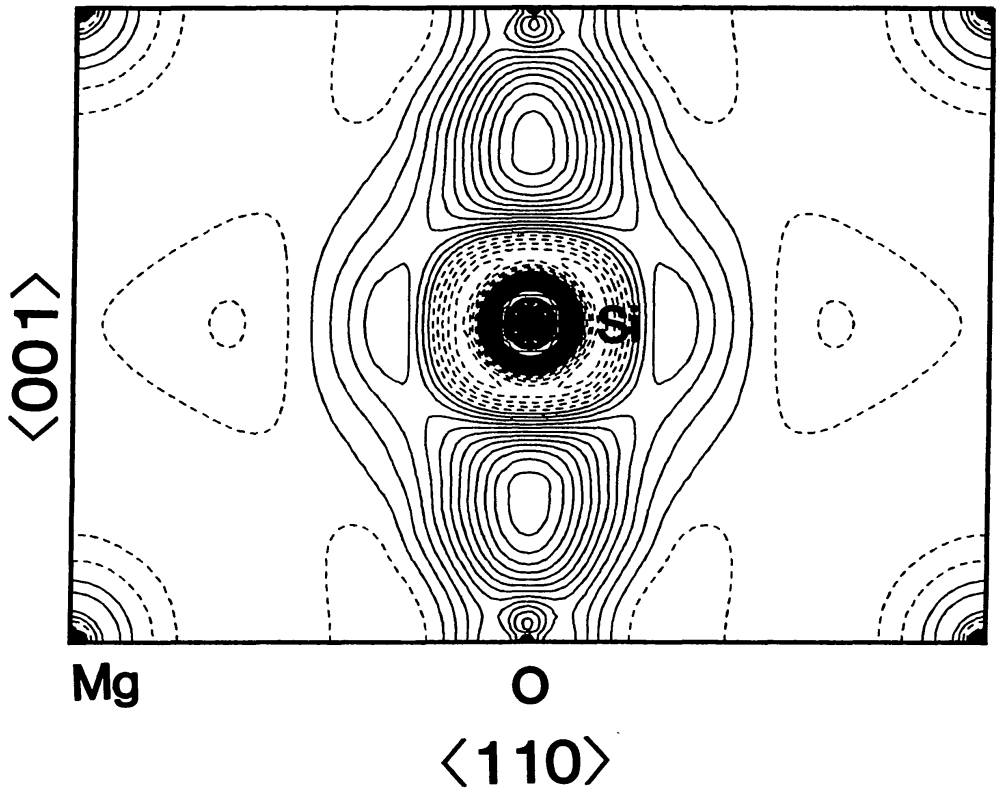

Figure 5 Difference between self-consistent LAPW charge density and overlapping spherical ions (Mg^{2+}, Si^{4+}, O^{2-}) for cubic $MgSiO_3$ along the (*110*) plane ($P = 155$ GPa). The contour interval is 0.005 $e^-/bohr^3$. Negative contours are dashed (from Cohen et al 1989).

STABILITY AND PHASE RELATIONS

The possibility that silicates may adopt a perovskite-type structure at high pressures was suggested by Ringwood (1962) on the basis of crystal chemical systematics. A variety of studies of high-pressure silicate perovskite analogues were carried out by Ringwood's group in the late 1960s (see Reid & Ringwood 1975). The formation of a perovskite-structured silicate was first demonstrated by Liu (1974, 1975a,b) in ferromagnesian silicates using the diamond-anvil cell. Subsequent to the discovery of $(Mg,Fe)SiO_3$ perovskite, considerable effort was directed toward understanding its stability field as a function of composition (Yagi et al 1977, Ito 1977). The phase relations in the pseudo binary systems Mg_2SiO_4-Fe_2SiO_4 and $MgSiO_3$-$FeSiO_3$ are shown in Figure 6, and the effect of pressure on the MgO-FeO-SiO_2 ternary diagram is presented in Figure 7. The composition range in which $(Mg,Fe)_2SiO_4$ spinel dissociates into perovskite and magnesiowüstite (Mg,Fe)O extends over the range

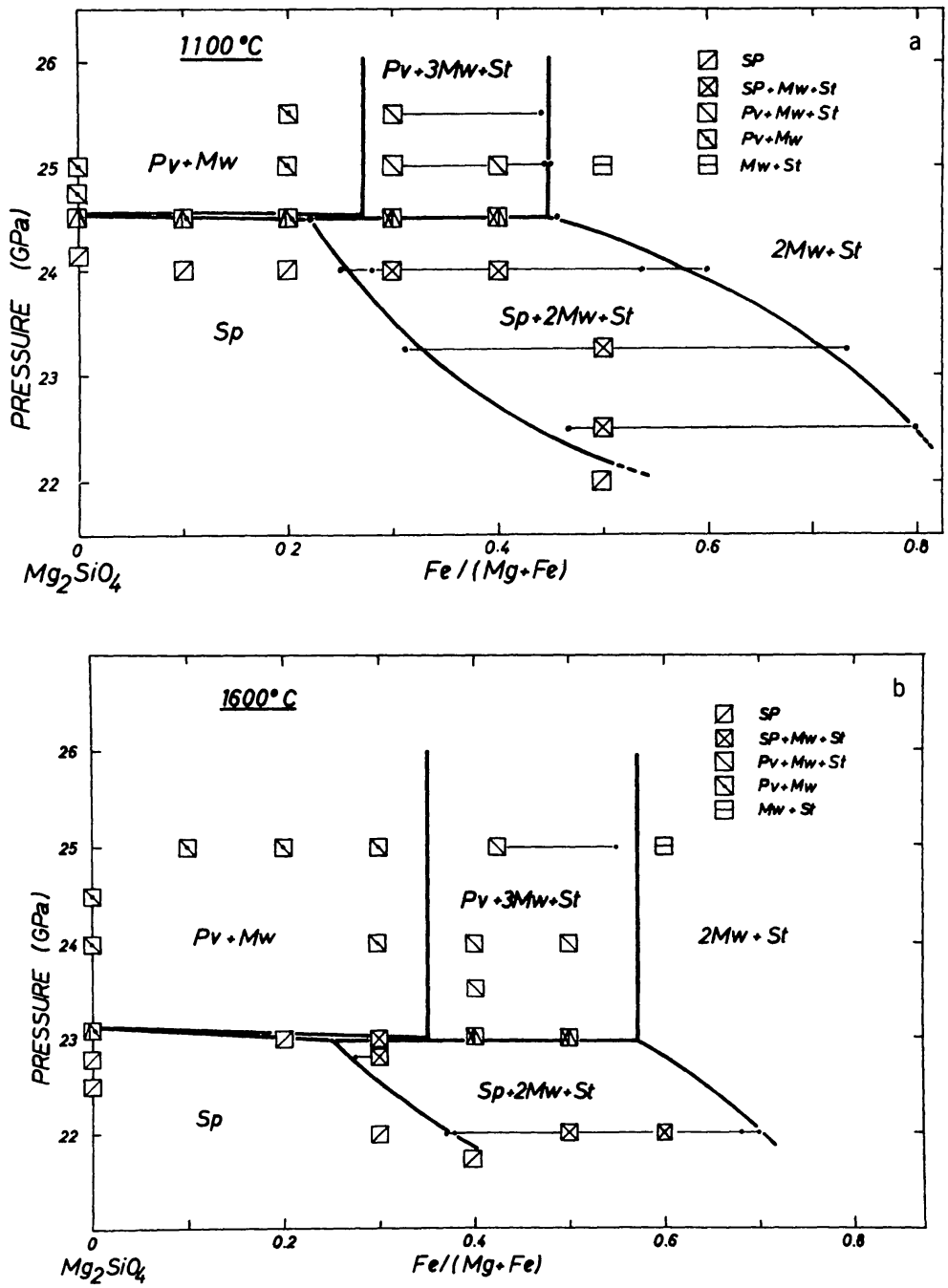

Figure 6 Pseudobinary diagrams in the system Mg_2SiO_4-Fe_2SiO_4 at 1373 K and 1873 K. Sp, spinel; Mw, magnesiowüstite; St, stishovite; Pv, perovskite (from Ito & Takahashi 1989).

Fe/(Mg+Fe) = 0 to 0.22; it thus covers the range of likely mantle compositions (Ringwood 1975, Anderson 1989). Yagi et al (1979c) performed phase equilibrium studies on laser-heated diamond-cell samples quenched from high pressures and temperatures. The experiments showed that the

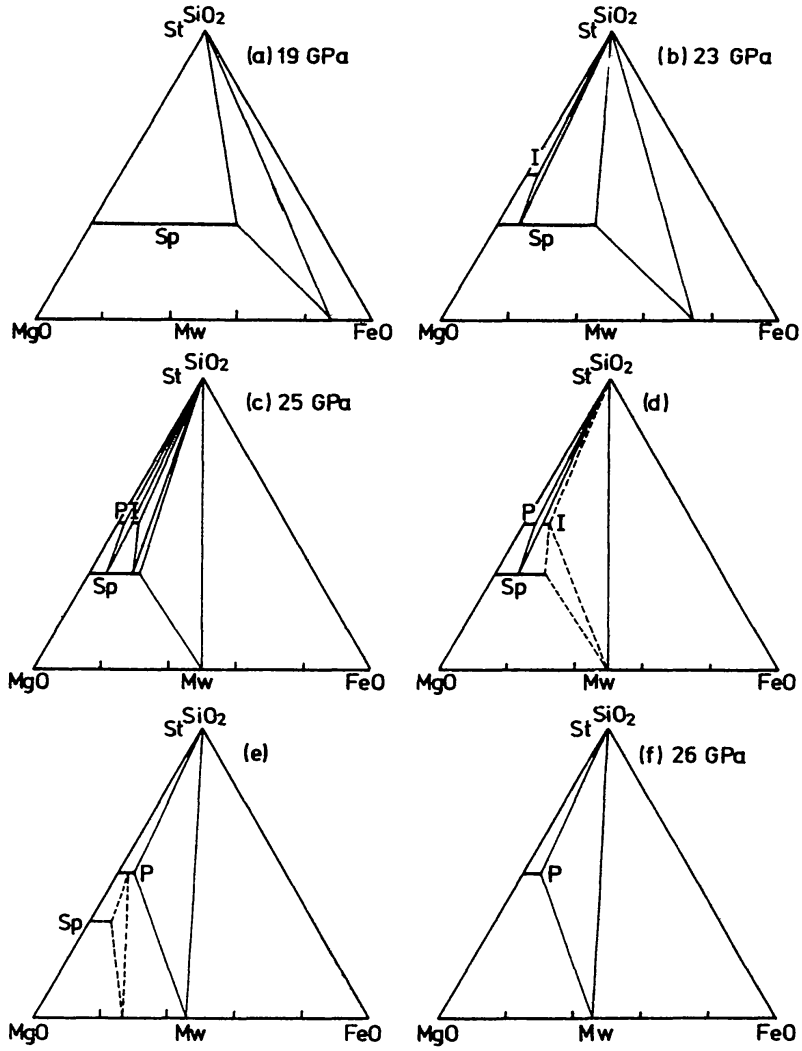

Figure 7 Ternary diagrams in the system FeO-MgO-SiO_2 as a function of pressure from 19 GPa to 26 GPa at 1373 K. Sp, spinel; Mw, magnesiowüstite; St, stishovite; I, ilmenite; Pv, perovskite (from Ito 1984).

three-phase loop of spinel, magnesiowüstite, and stishovite is very narrow in pressure, in fact narrower than the resolution of the experiments at that time. This result has been confirmed in more detailed phase equilibria studies with a large-volume multi-anvil press (Ito & Takahashi 1989), in which phase relations topologically close to those of the earlier studies were also found. There is now strong evidence that the dissociation reaction occurs within 0.2 GPa at ~1870 K, which corresponds to less than 4–6 km depth within the Earth (Wood 1990, Fei et al 1991b, Kuskov & Panferov 1991). The pressure of the disproportionation reaction and its sharpness

has important implications for the interpretation of the 670-km discontinuity, which can be explained as the result of the phase transition without the requirement of a change in chemical composition at this depth (see below).

Despite the emerging consensus on certain aspects of the phase relations in this system, several outstanding problems remain. In the diamond-cell experiments, the Pv+3Mw+St three-phase field (Figure 7) extends to higher FeO content than is indicated by the multi-anvil experiments (Ito & Takahashi 1989). The latter workers also find that the three-phase triangle moves toward more FeO-rich compositions with increasing temperature. However, attempts to model this behavior based on available thermochemical data show the opposite effect of temperature (Fei et al 1991b). The difference in maximum solubility of Fe in perovskite determined in diamond-cell and multi-anvil experiments is not yet resolved; possible differences in ferric iron content need to be examined (Fei et al 1991b, Hirsch & Shankland 1991). Guyot et al (1989) have obtained evidence for a pressure effect on the partitioning of iron between perovskite and magnesiowüstite. Preliminary measurements of the spinel to perovskite transition carried out in situ in a CO_2-laser-heated diamond-cell suggest that the *P-T* boundary could be up to 300°C higher than that determined in the multi-anvil quench experiments (Boehler & Chopelas 1991, 1992).

Another important problem in the phase diagram is the negative *P-T* (Clapeyron) slope of perovskite-forming transitions, which has important geophysical implications because if dP/dT is sufficiently negative it could inhibit mixing of the upper and lower mantle. Phase equilibrium and calorimetric data now indicate that the slope of the Il → Pv and Sp → Pv+Mw transitions is negative (Ito & Yamada 1982; Ito & Takahashi 1987a, 1989; Ito et al 1990). The value of dP/dT is approximately −0.004 GPa/K (Ito et al 1990), which is close to the value needed to preclude two-layer convection according to the calculations of Christensen & Yuen (1984). The value reported by Ito et al (1990) requires information on the relative thermal expansivities of the phases at high *P* and *T*. The results are most consistent with the phase equilibrium data of Ito & Takahashi (1989) if a zero-pressure thermal expansion coefficient $\alpha = 2.2 \times 10^{-5}\,K^{-1}$ is assumed (see below). Recent simulations of mantle convection show that intermittent mixing of the upper and lower mantle is possible if dP/dT has an intermediate value of −0.002 GPa/K (Machetel & Weber 1991).

A major question with regard to the presence of silicate perovskite throughout the lower mantle is the pressure range of its stability. Diamond-cell studies of quenched material by Mao et al (1977) indicated that $(Mg,Fe)SiO_3$ perovskite is stable to at least 60 GPa. It was these experiments that first gave rise to the experimentally-based proposal that

$(Mg,Fe)SiO_3$ perovskite may be the most abundant mineral in the Earth. More recently, Knittle & Jeanloz (1987a) performed in situ x-ray diffraction measurements of $(Mg,Fe)SiO_3$ and found evidence for its stability to pressures above 100 GPa. The range for stability of the perovskite as a function of *P-T-X* has not been studied in detail at very high pressures (e.g. >50 GPa), however. The stability of the perovskite phase relative to simple oxides is derived from its 2% higher density relative to the oxide assemblage under ambient conditions, but a possible perovskite breakdown under very high *P-T* conditions (e.g. *D″* region) needs to be examined (even in the absence of iron) because the relative densities under these conditions are poorly known (see below). Fei et al (1991a) have examined available thermochemical data for $(Mg,Fe)SiO_3$ and delineated the conditions under which it may break down to simple oxides at high *P* and *T*. On the basis of calculations of the melting curve, Stixrude & Bukowinski (1990) propose that $MgSiO_3$ breaks down to simple oxides at the *P-T* conditions of *D″* and thus may be responsible for seismic structure at the base of the lower mantle, although later calculations find a greater stability for the perovskite phase (Stixrude & Bukowinski 1992). These proposals need to be examined by direct experimental investigation. Little is known about the chemistry of the perovskites at deep mantle conditions (including the *D″* region), as detailed phase equilibrium studies need to be performed under these ultrahigh pressures. Nevertheless, there is evidence for new pressure-induced reactions under these conditions, for example, reactions between perovskite and molten iron above 70 GPa (Knittle & Jeanloz 1989b, 1991).

Liu & Ringwood (1975) reported the synthesis of cubic $CaSiO_3$ perovskite at 16 GPa, which was found to be nonquenchable. More recent work has established that the calcium perovskite forms at significantly lower pressure than does the magnesium perovskite (11–13 GPa) (Mao et al 1989a, Chen et al 1989, Tarrida & Richet 1989, Tamai & Yagi 1989, Irifune et al 1989). Recent in situ x-ray diffraction measurements have shown that the perovskite phase of $CaSiO_3$ is stable and retains its cubic structure to at least the pressure of the core-mantle boundary (Mao et al 1989a). Similar results have been obtained by Tarrida & Richet (1989) and Yagi et al (1989) to 94 GPa and above 100 GPa, respectively. The wide stability field of the cubic form is in general agreement with theoretical predictions (Hemley et al 1985, 1987; Wolf & Bukowinski 1987). The sharpness of diffraction lines rules out the possibility of tetragonal or orthorhombic distortion of more than 0.5%. The predicted pressure-induced distortion to a lower symmetry perovskite structure must take place at still higher pressures. Like the magnesium-rich perovskite, the temperature range of stability of the calcium perovskite has not been determined in detail

experimentally, and analysis of available equations of state shows that free energy of the oxide assemblage is very close to that of perovskite at very high pressures (Mao et al 1989a, Fei et al 1991a). During release of pressure, the perovskite persists metastably at pressures close to ambient. Near zero pressure, however, the phase could be preserved for only a few hours, although small quantities have been observed recently to persist over longer time periods (Kanzaki et al 1991). The observation of amorphization on decompression may be related to theoretical predictions that $CaSiO_3$ perovskite becomes dynamically unstable on expansion of the structure (Hemley & Cohen, unpublished).

Several experimental studies indicate very limited solubility between $(Mg,Fe)SiO_3$ and $CaSiO_3$-perovskite (Liu 1977; Mao et al 1977; Weng et al 1982; Irifune & Ringwood 1987a,b; Tamai & Yagi 1989, Irifune et al 1989). Diopside ($CaMgSi_2O_6$) breaks down to form orthorhombic Mg-rich and cubic Ca-rich perovskites above 24 GPa rather than a single perovskite phase. For example, Irifune et al (1989) report $<2\%$ solubility of $CaSiO_3$ in $MgSiO_3$ and 2–5% solubility of $MgSiO_3$ in $CaSiO_3$. By contrast, Liu (1987) reported complete solid solution between $CaSiO_3$ and $CaMgSi_2O_6$ in the cubic perovskite structure, and evidence for cubic perovskite with a nearly ideal diopside composition formed in garnet peridotite has been reported (Ito & Takahashi 1987a, Takahashi & Ito 1987). The differences could be associated with problems with metastability. Kim et al (1991) report formation of Ca-perovskite from hedenbergite ($CaFeSi_2O_6$) at 19–26 GPa. Silicate perovskites containing heavier alkaline earths Sr and Ba are predicted theoretically to be dynamically stable but only at high pressure (Hemley & Cohen, unpublished); the calculations indicate that they become dynamically unstable on decompression because of the large cation in the A site and therefore may be unquenchable from high pressures and temperature.

There have been limited reconnaissance studies of the phase relations involving a wider range of compositions (cf. Liu & Bassett 1986). A very important component is Al_2O_3. As discussed above, Weng et al (1982) showed that Al_2O_3 dissolves in magnesium perovskite up to 25 mole % instead of forming another phase such as garnet. Recently, a new high-pressure rhombohedral perovskite phase with composition $Ca_2AlSiO_{5.5}$ was reported by Fitz Gerald & Ringwood (1991). Solubility of alkali elements (e.g. Na) in silicate perovskite has been reported and the resulting phases generally appear to be nonquenchable. For example, Liu (1980, 1987) report evidence for the formation of a nonquenchable, cubic perovskite phase of omphacite composition. Experimental studies of the partitioning of transition metals between Mg-perovskite and metallic iron at high pressures have begun (Ohtani et al 1992; see also Knittle & Jeanloz

1989b, 1991). The solubility of hydrogen and rare gases in perovskite at high pressure is of great importance but remains to be determined.

PRESSURE-VOLUME RELATIONS

Measurement of the P-V equation of state is essential for geophysical models because such data in principle provide a determination of density ρ and bulk modulus K_S (or K_T), or bulk sound velocity $V_B = K_S/\rho$ as functions of pressure. The isothermal and adiabatic bulk moduli are related as: $K_S = K_T(1+\alpha\gamma T)$, where α is the volume thermal expansion coefficient and γ is the Grüneisen parameter. One of the advances in research on silicate perovskites during the past five years has been the direct measurement of the P-V relations for both $(Mg,Fe)SiO_3$ and $CaSiO_3$ perovskite over most of the pressure range of the lower mantle (>100 GPa). Figure 8 summarizes these results. A comparison of recent equation of state parameters for $(Mg,Fe)SiO_3$ is given in Table 1.

Yagi et al (1979b, 1982) first measured the P-V equation of state of $MgSiO_3$ by static compression under hydrostatic conditions using x-ray diffraction; they reported a value of the zero-pressure bulk modulus K_{0T} of 258($\pm$20) GPa ($dK_{0T}/dP \equiv K'_{0T} = 4$ assumed). The maximum pressure in this early study was 8 GPa—well below the stability field of the perovskite. Knittle & Jeanloz (1987a) measured the equation of state of $(Mg_{0.9}Fe_{0.1})SiO_3$ perovskite to pressures in excess of 100 GPa by x-ray diffraction of laser-heated samples (without a pressure medium). The x-ray diffraction patterns were indexed as orthorhombic perovskite. A third-order Birch Murnaghan equation-of-state fit to the data gave zero-pressure parameters $K_{0T} = 266(\pm 6)$ GPa and $K'_{0T} = 3.9(\pm 4)$. Subsequent static compression measurements have been carried out using single-crystal x-ray diffraction under hydrostatic conditions but at lower pressures. Kudoh et al (1987) report a lower value of $K_{0T} = 247$ GPa whereas Ross & Hazen (1990) find $K_{0T} = 254(\pm 13)$ GPa. Recent high-resolution powder diffraction measurements using synchrotron radiation to 30 GPa by Mao et al (1991) give $K_{0T} = 261(\pm 4)$. In each of these studies $K'_{0T} = 4$ was assumed. Yeganeh-Haeri et al (1989a,b) report a value for the adiabatic bulk modulus K_{0S} of 246($\pm$1) GPa on the basis of single-crystal Brillouin scattering spectroscopy carried out at zero pressure; the value for K_{0T} calculated from this result is 243($\pm$1) GPa (see below). Recent results indicate that, within experimental uncertainties, the bulk moduli of $Mg_{1-x}Fe_xSiO_3$ perovskites, with $x = 0$, 0.1, and 0.2, are independent of x (Mao et al 1989b, 1991). Therefore, the density of perovskite at high pressure increases with x in proportion to the density dependence of x at zero pressure (Figure 2).

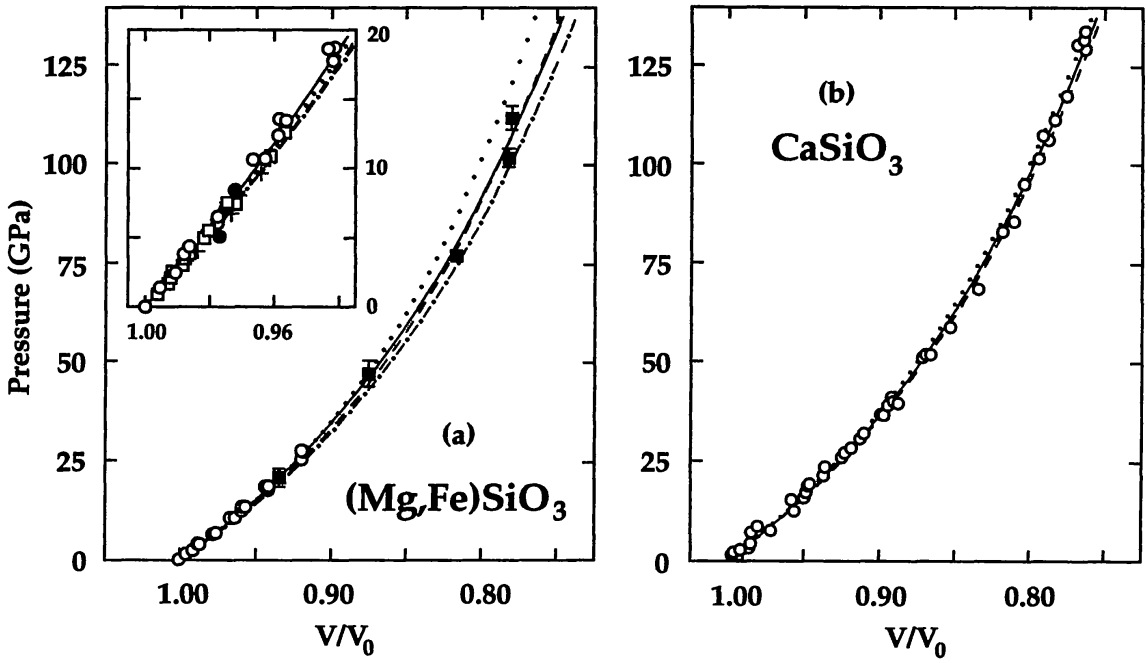

Figure 8 Static compression data and *P-V* equations of state for silicate perovskites (room temperature). The experimental points are from high-pressure x-ray diffraction measurements and the curves represent least-squares fits to different data sets using Birch-Murnaghan finite-strain equations of state (see text and Table 1). (*a*) $(Mg,Fe)SiO_3$-peroskite: ●, Yagi et al (1982); +, Kudoh et al (1987); ■, Knittle & Jeanloz (1987); □, Ross & Hazen (1990); ○, Mao et al (1991). (*Solid line*) $K_{0T} = 266(\pm 6)$ GPa and $K'_{0T} = 3.9(\pm 0.4)$ (Knittle & Jeanloz 1987a), and $K_{0T} = 261(\pm 4)$ GPa and $K'_{0T} = 4$ assumed (Mao et al 1991); these curves are indistinguishable on this scale; (*dotted dashed line*) $K_{0T} = 246$ GPa and $K'_{0T} = 4$ assumed (Kudoh et al 1987; see also Yeganeh-Haeri et al 1989a,b; Chopelas & Boehler 1989); (*dashed line*) $K_{0T} = 246$ GPa and $K'_{0T} = 4.5$ (e.g. Stixrude & Bukowinski 1992); (*dotted line*) $K_{0T} = 246$ GPa and $K'_{0T} = 5.5$ (see Mao et al 1991). The unit-cell volumes are given in Figure 2. (*b*) $CaSiO_3$ perovskite: ○, Mao et al (1989a). (*Solid line*) $V_0 = 45.31(\pm 0.08)$ Å^3 (per unit cell), $K_{0T} = 281(\pm 6)$ GPa, $K'_{0T} = 4$ assumed (Mao et al 1989a); (*dashed line*) $V_0 = 45.60(\pm 0.10)$ Å^3, $K_{0T} = 275(\pm 15)$ GPa, $K'_{0T} = 4$ assumed (Tarrida & Richet 1989); (*dotted line*) $V_0 = 45.58(\pm 0.07)$ Å^3, $K_{0T} = 288(\pm 13)$ GPa, $K'_{0T} = 4$ assumed (Yagi et al 1989). Agreement among the three studies is very good; for clarity only the data points from Mao et al (1989a) are shown.

Although these differences in the bulk moduli determinations are perhaps typical of inter-laboratory comparisons, particularly for incompressible materials and different techniques, they nevertheless have important geophysical implications because they can give rise to significant differences in extrapolated values for the density (and bulk sound velocity) of perovskites at lower-mantle pressures. Some of these apparent discrepancies can be removed by recognizing the trade-off between K_{0T} and K'_{0T} in equation-of-state fits to the data (Mao et al 1991). For example,

to reconcile the low bulk modulus obtained from Brillouin scattering (Yeganeh-Haeri et al 1989a,b) with the high-resolution diffraction data of Mao et al (1991), a relatively high value for $K'_{0T} \sim 5.5$ must be assumed (Mao et al 1991). The high K'_{0T} however, is inconsistent with the higher pressure diffraction data of Knittle & Jeanloz (1987a) (see Hemley et al 1992) (Figure 8a). A consistent set of pressure-volume relations is therefore only available for pressures corresponding to the top of the lower mantle (23 GPa to perhaps 50 GPa). At higher pressures, the differences become more pronounced, which adds uncertainty to constraints on mineralogy and composition of the lower mantle based on extrapolated equations of state, even in the absence of the thermal effects described below.

Comparison of recent measurements of the linear compressibilities of $(Mg,Fe)SiO_3$ perovskite are listed in Table 1. In general, the present conclusion that the *b*-axis is the least compressible is consistent with the zero-pressure Brillouin scattering study of $MgSiO_3$ perovskite by Yeganeh-Haeri et al (1989a,b) and single-crystal x-ray diffraction studies of $MgSiO_3$ perovskite by Kudoh et al (1987) and Ross & Hazen (1989). The remaining differences among these results may be explained as uncertainties associated with the smaller pressure range of study for the single-crystal data, although structural differences between the $(Mg,Fe)SiO_3$ synthesized in diamond-anvil cells and in large-volume apparati cannot be ruled out. It is possible, for example, that this is associated with different amounts of ferric iron (Fe^{+3}) formed due to differences in oxygen fugacity in the two types of experiments (Fei et al 1991b). Nonhydrostatic pressure has a major effect on the relative compressibilities of lattice parameters. In addition, without the resolution to separate the orthorhombic splitting of the equivalent cubic diffraction peaks, relative compressibilities of lattice parameters could not be accurately determined.

The room temperature *P-V* equation of state of $CaSiO_3$ has been measured by x-ray diffraction in diamond-cells to pressures in the 100 GPa range by three groups (Mao et al 1989a, Yagi et al 1989, Tarrida & Richet 1989). The results are shown in Figure 8*b*. The agreement is comparable to that observed for $(Mg,Fe)SiO_3$ equation of state studies. The similar values for the bulk moduli of the two perovskites has lead to the proposal that $CaSiO_3$ perovskite could be an invisible component in the lower mantle (Mao et al 1989a, Tarrida & Richet 1989).

THERMAL EXPANSION

Because of the high temperatures prevailing in the lower mantle (>1700 K, e.g. Jeanloz & Morris 1986), determination of the thermal expansivity of silicate perovskite is essential for estimation of the density (and bulk

modulus) of the material within the Earth. The critical role of the thermal expansivity of the material for controlling chemical layering and the style of convection within the mantle was pointed out by Jackson (1983) and Jeanloz & Thompson (1983). Figure 9 summarizes the results of thermal expansion studies of $(Mg,Fe)SiO_3$ perovskite at zero pressure. Knittle et al (1986) measured the thermal expansion from 300–870 K at zero pressure of polycrystalline $(Mg_{0.9}Fe_{0.1})SiO_3$ perovskite synthesized in a diamond-cell and obtained a value for the volume thermal expansion coefficient α exceeding 4×10^{-5} K^{-1} above 500 K. Ross & Hazen (1989) measured the thermal expansion at low temperatures (77–400 K), and more recently Parise et al (1990) performed powder diffraction measurements from 10 to 433 K. These studies have provided accurate determination of the thermal expansivity, with $\alpha = 1.9$–2.1×10^{-5} K^{-1} at 300 K, but they are

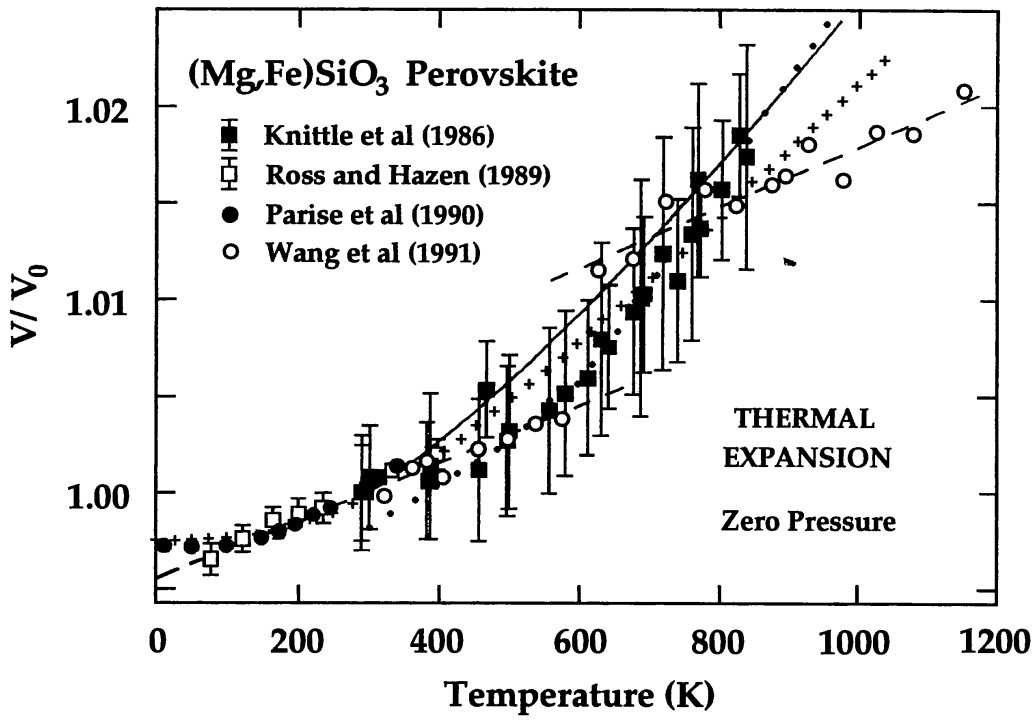

Figure 9 Relative volume of $(Mg,Fe)SiO_3$ perovskite as a function of temperature at zero-pressure (V_0 is the room-temperature volume). Knittle et al (1986) studied $(Mg_{0.9}Fe_{0.1})SiO_3$ composition; Ross & Hazen (1989), Parise et al (1990), and Wang et al (1991a) examined the $MgSiO_3$ endmember. The lines are fits to the experimental data: (*dotted line*) Knittle et al (1986), Grüneisen-Suzuki model fit to the high-temperature data, with $V_0 = 162.25$ Å^3, $K_0 = 260$ GPa, $K'_{0T} = 4$, $\Theta_D = 825$ K, and $\gamma_D = 2.20$; (*solid line*) Mao et al (1991), obtained from fitting high-P-T data, with $\alpha = 0.301 \times 10^{-4} + 1.500 \times 10^{-8}\ T - 1.139\ T^{-2}$ (zero pressure); (+ + + +) Stixrude & Bukowinski (1990), Mie-Grüneisen-Debye model fit to zero-pressure thermal expansivity and phase equilibria data, $V_0 = 162.25(\pm 0.05)$ Å^3, $\Theta_D = 1016(\pm 6)$ K, and $\gamma_D = 1.73(\pm 0.14)$; (*dashed line*) Wang et al (1991a), linear fit showing proposed phase transition at 600 K.

limited to relatively low temperatures. The results are compatible with the higher thermal expansion found by Knittle et al (1986) if one assumes a temperature dependent α, as found for other silicates. There has been concern, however, since these measurements of thermal expansivity (as well as other properties) were made well outside the perovskite stability field (Navrotsky 1989, Hill & Jackson 1990) where the phase is very unstable. Wang et al (1991a) have reported that $MgSiO_3$ perovskite undergoes a metastable phase transition at 600 K and 7.1 GPa, which is responsible for the high thermal expansivity observed at low pressures (Figure 7); this is discussed in further detail below. Very recently, Wang et al (1991b) reported low thermal expansivities which they attribute to partial conversion to an amorphous phase at zero pressure. Hence this topic continues to be a subject of debate.

A variety of models have been used to examine this question. The Grüneisen parameter can be used to evaluate the thermal expansivity (or thermal pressure) using the thermodynamic Grüneisen parameter defined as $\gamma_{th} = \alpha K_T V/C_V$. Constraints on γ_{th} for silicate perovskites have been obtained from high-pressure vibrational spectra described below (Williams et al 1987, Hemley et al 1989) and from direct fits to high-temperature expansivity data (Knittle et al 1986, Jeanloz & Knittle 1989, Stixrude & Bukowinski 1990, Hemley et al 1992). Simple thermal models such as Einstein and Debye approximations have been used, including the formalism developed by Suzuki (1975) based on Grüneisen theory (Knittle et al 1986). These models involve a parameterization of the thermal pressure with a single characteristic frequency, together with a Grüneisen parameter γ_D, defined as $\gamma_D = -d\ln\Theta_D/d\ln V$, and possibly higher-order terms, where Θ_D is an effective Debye temperature, which is equivalent to the Einstein temperature ($\Theta_D = \sqrt{5/3}\Theta_E$) for $T > \Theta_D$. One of the problems is that γ_{th} is not determined directly in these studies: The γ_D and that determined by spectroscopic data need not be the same as the thermodynamic Grüneisen parameter γ_{th}. Nevertheless, both the spectroscopic data and independent theoretical predictions indicate that γ_{th} is 1.7–2.0 (Williams et al 1987, Hemley et al 1989, Hemley 1991), which is higher than is typically found for other materials (silicates and oxides), consistent with the γ_D determined from the thermal expansivity data (Knittle et al 1986). Estimates of Θ_D range from 725 to 1200 K (Knittle et al 1986; Wolf & Bukowinski 1987; Hemley et al 1987, 1989; Jeanloz & Knittle 1989; Stixrude & Bukowinski 1990); the range in estimates is due in part to the fact that the vibrational density of states is not well represented by a Debye model. Nevertheless, similar fits to the high-temperature thermal expansivity can be obtained over this range because of the trade-off in parameters (Hemley et al 1992). The problem has also been examined by the use of theoretical calculations

with nonempirical (ab initio) models (Hemley et al 1987, 1989; Cohen 1987; Wolf & Bukowinski 1987) and empirical approaches (Matsui 1988). The recent lattice dynamical models are not inconsistent with the experimentally observed expansivity, including its temperature dependence, but it should be noted that lattice dynamical predictions of thermal expansion are in general highly sensitive to the interatomic potentials.

The crucial property for comparison of the density of silicate perovskites and other possible lower mantle phases with seismological density profiles is the density at the relevant P-T conditions, which requires a knowledge of the variation in α with pressure as well as temperature. The variation in α with pressure is characterized by the Anderson-Grüneisen parameter $\delta_{T,S}$, which is defined as $\delta_{T,S} = -1/(\alpha K_{T,S})(dK_{T,S}/dT)$. Assuming $\delta_{T,S}$ is independent of P and T, it can be shown that $\delta_{T,S} = (d\ln\alpha/d\ln V)_P$. Constraints on this quantity have been obtained by the use of systematics developed at lower P and T for other materials (Chopelas & Boehler 1989, Anderson et al 1990, Bina & Helffrich 1992). Alternatively, theoretical models provide useful predictions of this quantity (Wolf & Bukowinski 1987, Hemley et al 1987, Isaak et al 1990). Jeanloz & Knittle (1989) developed empirical equations of state for both (Mg,Fe)SiO_3 and (Mg,Fe)O based on an anharmonic Einstein model, predicting the densities of both phases under lower-mantle pressures and temperatures.

Recently, the pressure dependence of α has been determined from direct measurements of the density of (Mg,Fe)SiO_3 at high pressures and temperatures by the use of x-ray diffraction techniques (Mao et al 1991). These results are summarized in Figure 10. The results support a high value for δ_T ($\sim$6.5) although measurements are not yet possible at lower-mantle temperatures (about 1700 K). Notably, these results are also consistent with the zero-pressure values for α reported by Knittle et al (1986). Because at the highest pressures the measurements were performed within the stability field of the perovskite, no problems with formation of an amorphous phase were encountered under these conditions. Since a decrease in δ_T is expected above the Debye temperature (e.g. Anderson et al 1990), it is important that these measurements be extended to higher temperatures (i.e. above 900 K). Extension of the measurements to higher pressures would also provide the direct determination of the pressure dependence of δ_T, which could be significant under deep lower mantle conditions (Isaak et al 1990).

SHEAR MODULUS

The shear modulus is an even more difficult quantity to measure than either the bulk modulus and equation of state, particularly at high pressures, and

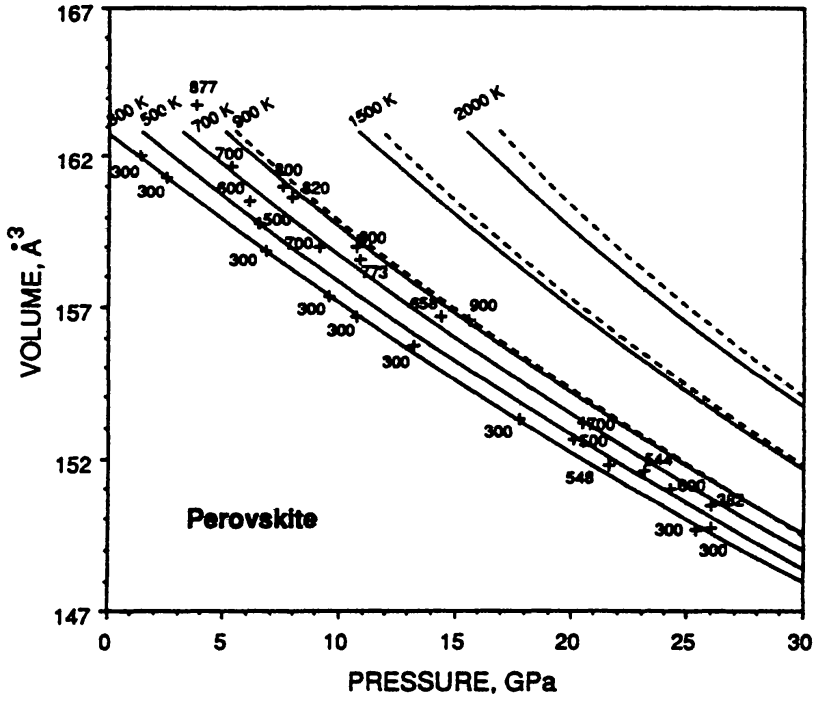

Figure 10 *P-V-T* relations for $(Mg,Fe)SiO_3$ perovskite. The curves were fits to the high *P-T* volume measurements (*points*) with $K_{0T} = 261$ GPa, $K'_{0T} = 4$. $\delta_T = 7.4$ (*dashed line*) and $\delta_T = 6.5$ (*solid line*) (from Mao et al 1991).

little was known about this quantity until recently. The shear modulus μ is important because primary seismological data give shear and longitudinal wave velocities (V_S and V_P), both of which depend on the shear modulus; i.e. $V_S = (G/\rho)^{1/2}$ and $V_P = [(K_S + 4/3G)/\rho]^{1/2}$. Predictions of G for silicate perovskite ranging from 140 to 190 GPa were made on the basis of crystal chemical systematics and theoretical models (e.g. Jeanloz & Thompson 1983, Cohen 1987, Matsui et al 1987). The high value of 190 GPa for $MgSiO_3$ perovskite under ambient conditions predicted theoretically using the PIB model (Cohen 1987) was subsequently confirmed by Brillouin scattering measurements of Yeganeh-Haeri et al (1989a,b), who reported a value of 184.2($\pm$4.0) GPa (both Voight-Reuss-Hill bounds). Table 2 lists the complete set of single-crystal elastic moduli from these two studies. One of the striking features of these results is that the value of G under room conditions is equivalent to that of the lower mantle at 1000 km depth (e.g. Dziewonski & Anderson 1981). If the lower mantle is predominantly perovskite, this result indicates that the pressure and temperature effects nearly completely offset each other at this depth (40 GPa and 1900–2300 K).

Table 2 Elastic constants (in GPa) for $MgSiO_3$ perovskite at zero pressure

	Theory[a]			Exp[b]
	c_{ij}		$\partial c_{ij}/\partial P$	c_{ij}
	Static	298K	298K	295 K
c_{11}	548	531	6.1	520
c_{12}	54	44	3.2	114
c_{22}	551	531	5.6	510
c_{13}	153	143	3.0	118
c_{23}	175	166	3.0	139
c_{33}	441	425	6.3	437
c_{44}	241	237	1.9	181
c_{55}	253	249	1.4	202
c_{66}	139	136	1.7	176
K	256	249	4.1	245
G	196	192	1.7	184

[a] Potential-induced breathing model (Cohen 1987).
[b] Brillouin scattering spectroscopy (Yeganeh-Haeri et al 1989a,b).

Although measurements of G under these P-T conditions are not yet possible, theoretical calculations can be used to assess the relative contributions of pressure and temperature. Given a model for the interatomic forces, the calculations of the pressure derivatives of the elastic moduli are straightforward and have been performed for $MgSiO_3$ perovskite (Cohen 1987). The calculation of the temperature derivatives (thermal elastic constants) are more difficult for low-symmetry structures where there are Raman-active modes, since the Raman modes couple with the elastic constants. At a pressure corresponding to 1071 km depth, $G = 255$ GPa (at 300 K), which indicates that $dG/dT \approx 0.04$ GPa/K to be consistent with geophysical data assuming a perovskite-dominated lower mantle (cf Yeganeh-Haeri et al 1989a). It should be pointed out that the effect of iron content on the shear modulus has not been determined and could be significant.

MELTING

Information on the melting curve and melting relations of silicate perovskites is central to a number of problems in solid-Earth geophysics. Melting

provides the most important mechanism for chemical differentiation in the Earth; hence, perovskite melting figures prominently in models of the early evolution of the planet. Because of the absence of widespread melting in the lower mantle, the determination of the solidus of silicate perovskite in principle provides an upper bound on the temperature distribution through a large fraction of the planet. In addition, measurement of the fusion curve provides bounds on the density of the liquid at high pressures and the extent to which ultrabasic liquids can become neutrally buoyant relative to surrounding crystalline phases at depth. Although virtually nothing was known about the melting of silicate perovskites just five years ago, there is now considerable information as a result of a series of pioneering experiments at the forefront of high *P-T* technology.

The results are shown in Figure 11. Heinz & Jeanloz (1987) reported diamond-cell measurements of the melting curve of $(Mg,Fe)SiO_3$ to 60 GPa and concluded that melting is independent of pressure above ~30 GPa ($T_m \sim 3000$ K). This curve was significantly lower than predictions based on empirical models and extrapolations of low-pressure data (Ohtani 1983, Poirier 1989). Subsequent measurements by Bassett et al (1988)

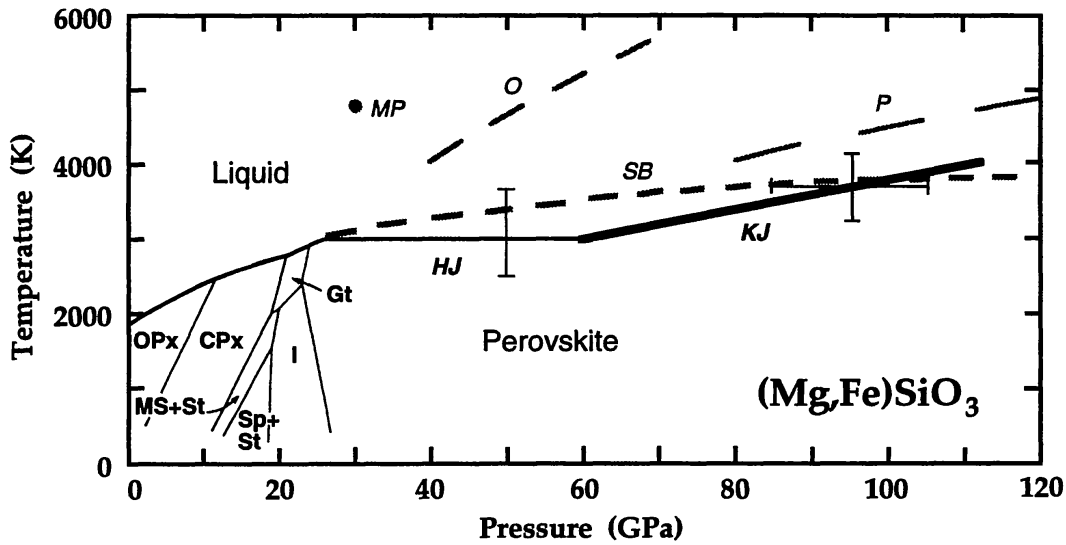

Figure 11 Melting curve for $(Mg,Fe)SiO_3$. The solid line (*HJ*) is the experimental result of Heinz & Jeanloz (1987) for $(Mg_{0.9}Fe_{0.1})SiO_3$ perovskite obtained to 60(±5) GPa, and the bold line at higher pressures (*KJ*) is the result of Knittle & Jeanloz (1989a) determined experimentally to 96(±10) GPa. The error bars give a measure of the estimated uncertainties in the measurements at the highest pressures (see original references for details). The dashed curves are calculated results for $MgSiO_3$ perovskite using a variety of methods: O—Ohtani (1983), P—Poirier (1989), SB—Stixrude & Bukowinski (1990), MP—Matsui & Price (1991). The lower pressure phase relations for $MgSiO_3$ composition are also shown (Kato & Kumazawa 1985).

support the Heinz & Jeanloz result. A higher pressure study by Knittle & Jeanloz (1989) indicates there may be a weak increase in T_m with pressure above 50 GPa. Ito & Katsura (1992) studied the melting of $MgSiO_3$ using a multi-anvil press and found T_m of 2870 K with a slope of 30 K/GPa, but the observations were limited to 21–25 GPa. Further measurements are certainly required. It is not known, for example, if the melting is congruent at very high pressures (Knittle & Jeanloz 1989a, Kubicki & Hemley 1989). Williams (1990) melted $(Mg_{0.88}Fe_{0.12})SiO_4$ in a laser-heated diamond-cell at 50–55 GPa. Infrared measurements of the quenched glasses show evidence for enrichment in SiO_2 with Mw as the liquidus phase. Ito & Katsura (1992) find eutectic melting between Mw and Pv, infer that eutectic composition shifts toward pyroxene composition with pressure, and suggest incongruent melting at deep mantle pressures.

A decrease in the melting slope with pressure indicates that the volume change on fusion approaches zero, which would require significant changes in liquid structure to take place over this pressure range. The extent to which such a change in liquid structure for $MgSiO_3$ compositions is associated with coordination changes in the liquid at these pressures has been a subject of continued discussion (Heinz & Jeanloz 1987; Knittle & Jeanloz 1989b; Jeanloz 1990; Miller et al 1991a,b). Early molecular dynamics simulations predicted a coordination change at very high compressions, although the actual pressures were not accurately determined (Matsui & Kawamura 1980, Matsui et al 1982). More recent simulations also predict this transition, but they also show that high densities can be reached without changes in Si coordination changes, i.e. by repacking of SiO_4 tetrahedra (Kubicki & Lasaga 1991). This result also seems to be consistent with high-pressure Raman studies, although these measurements have been limited to glasses at room temperature and may not be direct analogues of melts (Kubicki et al 1992). Stixrude & Bukowinski (1990) calculated the fusion curve from available thermochemical data (mostly at lower pressures). They find that a leveling off and possibly a maximum in the melting curve is compatible with the current data. However, the result is extremely sensitive to key parameters (such as the compressibility of the melt) which have not been measured at mantle conditions (Hemley & Kubicki 1991), so this result remains speculative. Recent molecular dynamics calculations of Matsui & Price (1991) predict a significantly higher melting curve, with no maximum under lower mantle conditions, which may be taken as evidence against neutral buoyancy of $MgSiO_3$ melts in the lower mantle. On the other hand, on the basis of recent shock-wave studies of komatiite liquid to 36 GPa, Miller et al (1991a,b) suggest that liquidus perovskite is neutrally buoyant at 70 GPa.

VIBRATIONAL DYNAMICS

The vibrational properties of perovskite are important for understanding the nature of possible distortions and for identifying phase transitions in these materials. In this regard, vibrational Raman scattering is particularly relevant because the activity of the first-order Raman spectrum is strongly dependent on the distortions of the crystal from the high-symmetry cubic form. This arises from the fact that all of the Raman-active vibrations in the distorted (e.g. orthorhombic) perovskite structures are derived from modes that occur at the edge of the Brillouin zone in the cubic form (cubic perovskite has no Raman-active modes). Certain of these modes are associated with displacive transitions between low and high-symmetry perovskite structures; that is, they may be soft modes, vibrations whose frequencies decrease and eventually vanish as a function of either pressure or temperature at the transition (cf. McMillan 1988).

There are 20 atoms in the primitive unit cell in *Pbnm* perovskite; thus there are 60 zone center modes including the 3 translational modes. The optic modes decompose as $7A_g+7B_{1g}+5B_{2g}+5B_{3g}+8A_u+7B_{1u}+9B_{2u}+9B_{3u}$. There are 24 Raman-active modes (A_g, B_{1g}, B_{2g}, and B_{3g}) and 25 infrared-active modes (B_{1u}, B_{2u}, and B_{3u}). The symmetry vibrations for orthorhombic *Pbnm* perovskite are shown in Figure 12.

The infrared spectrum of $MgSiO_3$ perovskite, first measured by Weng et al (1983) at zero pressure shows vibrations characteristic of octahedrally coordinated Si. Williams et al (1987) reported measurements of the pressure dependence of the infrared spectrum to 27 GPa as well as the Raman spectrum at zero pressure. Hemley et al (1989) measured the pressure dependence of the Raman spectrum of single crystals of $MgSiO_3$, and recently Chopelas & Boehler (1992) measured spectra of polycrystalline samples. The pressure dependences of the vibrational modes documented in these studies are shown in Figure 13. Additional preliminary data on the pressure dependence of the far-infrared spectrum have been reported (Hofmeister et al 1987, see also Hemley et al 1989). No soft-mode behavior was observed in any of the high-pressure measurements. Chopelas & Boehler (1992) report a decrease in intensity and a small change in pressure shifts of two modes at 37 GPa, which they have interpreted as evidence for a phase transition. However, no transition has yet been observed by x-ray diffraction in this pressure range, as discussed above. In general there is considerable coupling of the polyhedral vibrations in the perovskite. This strong coupling of the modes is associated with characteristic face-sharing of the component polyhedra (SiO_6 octahedra and MgO_{12} distorted dodecahedra). The observed vibrational modes have not yet been assigned

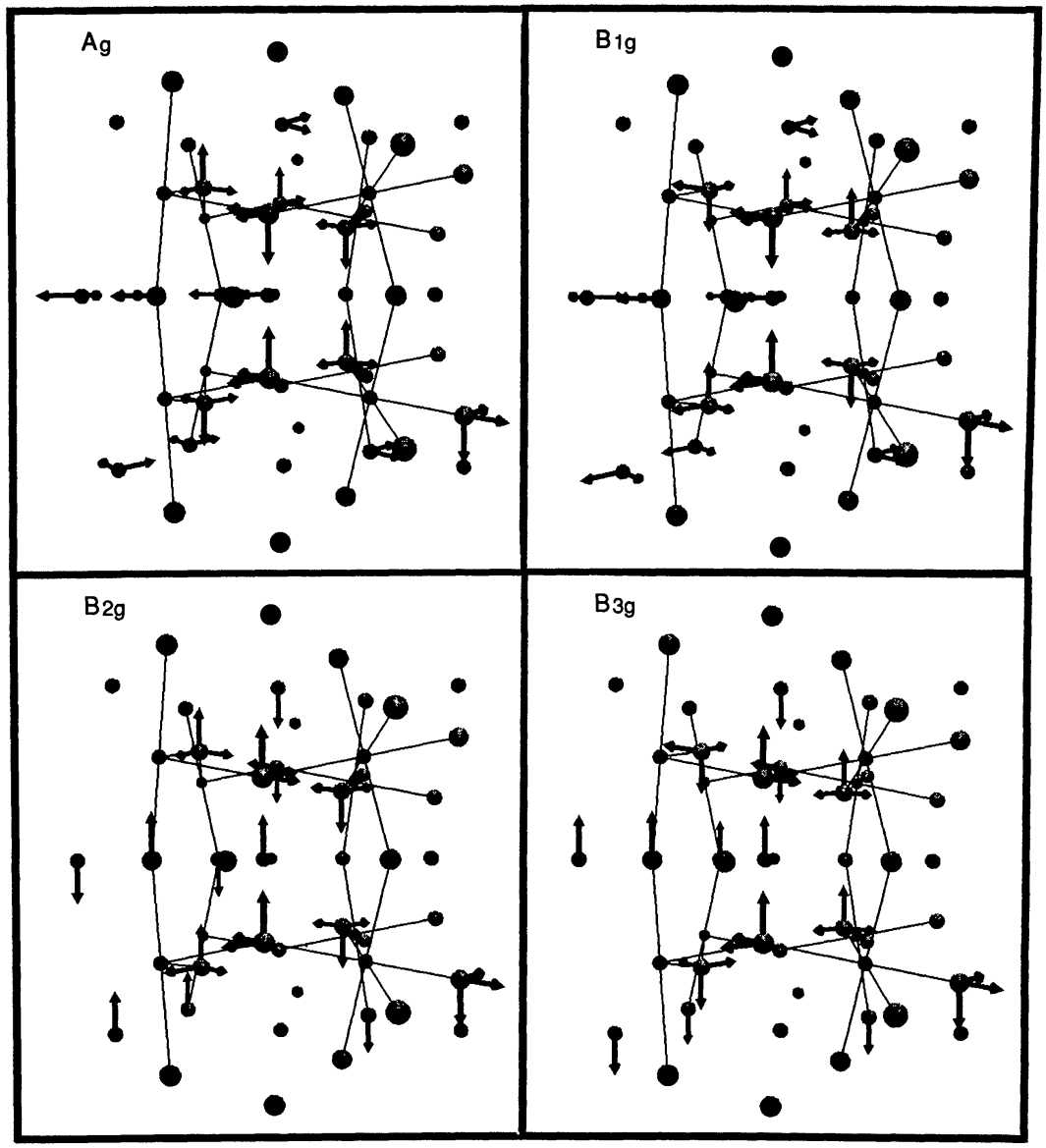

Figure 12 (*a*) Raman-active symmetry modes for *Pbnm* perovskite. The view is along (*110*) in the orthorhombic cell, or (*100*) in cubic coordinates. The *c*-axis is vertical. Si-O "bonds" are indicated by solid lines. The arrows indicate the atomic displacements for each type of symmetry mode. Only the minimum number of displacement vectors are shown, and the displacements are copied by unit-cell translations. The actual vibrational modes are linear combinations of the motions shown. Thus for A_g there are 7 modes, which are linear combinations of O(1) and Mg displacements in the *x*- and *y*-directions, and O(2) displacements in the *x*-, *y*-, and *z*-directions. Only the A_g symmetry modes correspond to possible tilt transitions. (*b*) Odd-symmetry modes for *Pbnm* perovskite. The A_u modes are inactive, and the B_{1u}, B_{2u}, and B_{3u} are infrared active. All of these modes break inversion symmetry, but only the *B* modes generate a dipole moment that can interact with infrared radiation.

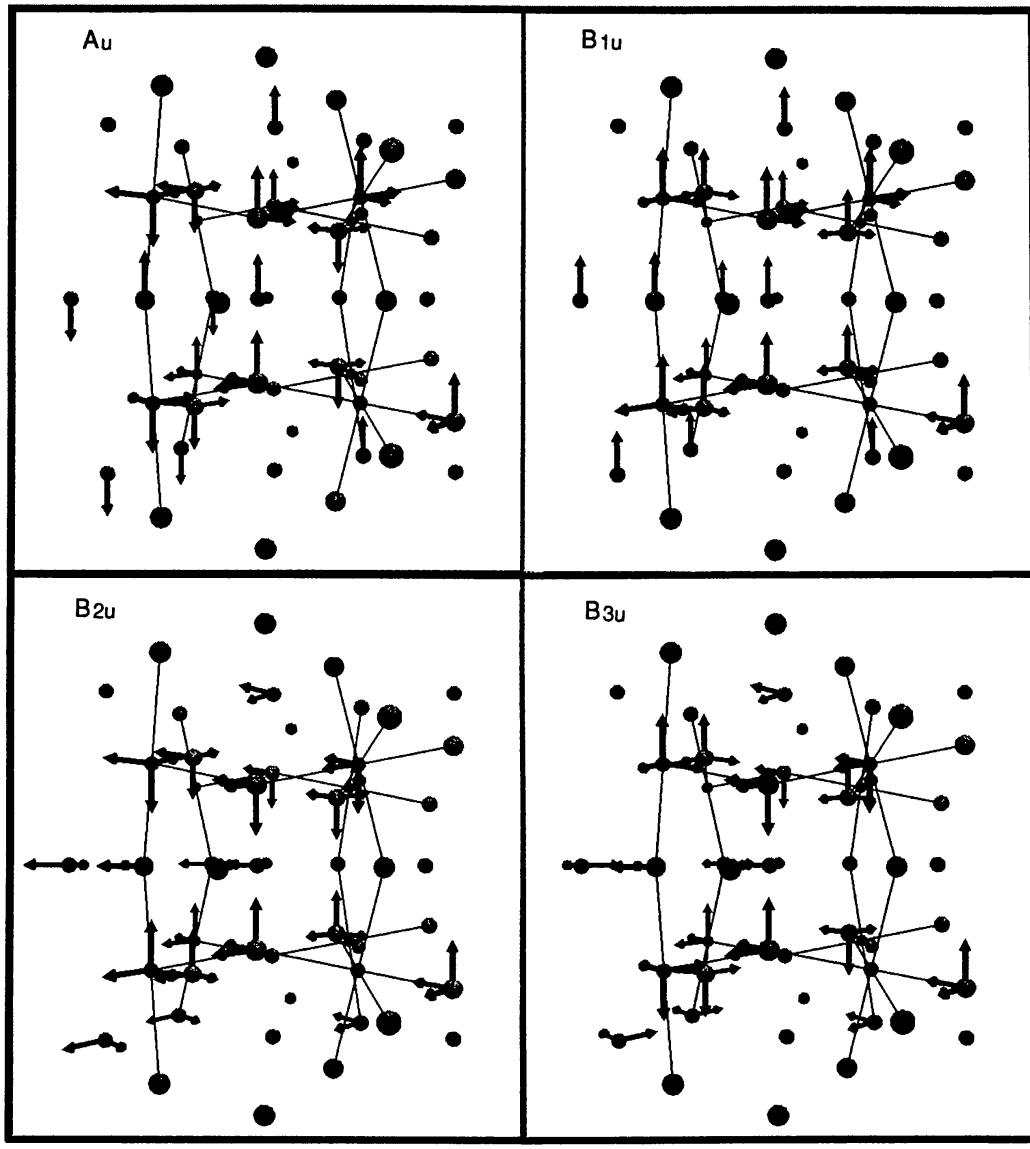

Figure 12b

to specific symmetry species, although it is likely that the strongest Raman bands have A_g symmetry.

Mode-Grüneisen parameters γ_i can be obtained from least-squares fits of the high-pressure mid-infrared and Raman data (Williams et al 1987, Hemley et al 1989, Chopelas & Boehler 1992). This information is important for assessing the microscopic origin of thermodynamic properties such as thermal expansivity and entropy. The γ_{0i} (values at zero pressure) are comparatively large, which indicates that the material has appreciable anharmonicity, at least at low pressure. The results can be used to calculate the Grüneisen parameter via the approximation, $\gamma_{th} \approx \langle \gamma_i \rangle = \Sigma \gamma_i c_i / \Sigma c_i$, where c_i is the heat capacity function for an Einstein oscillator and the

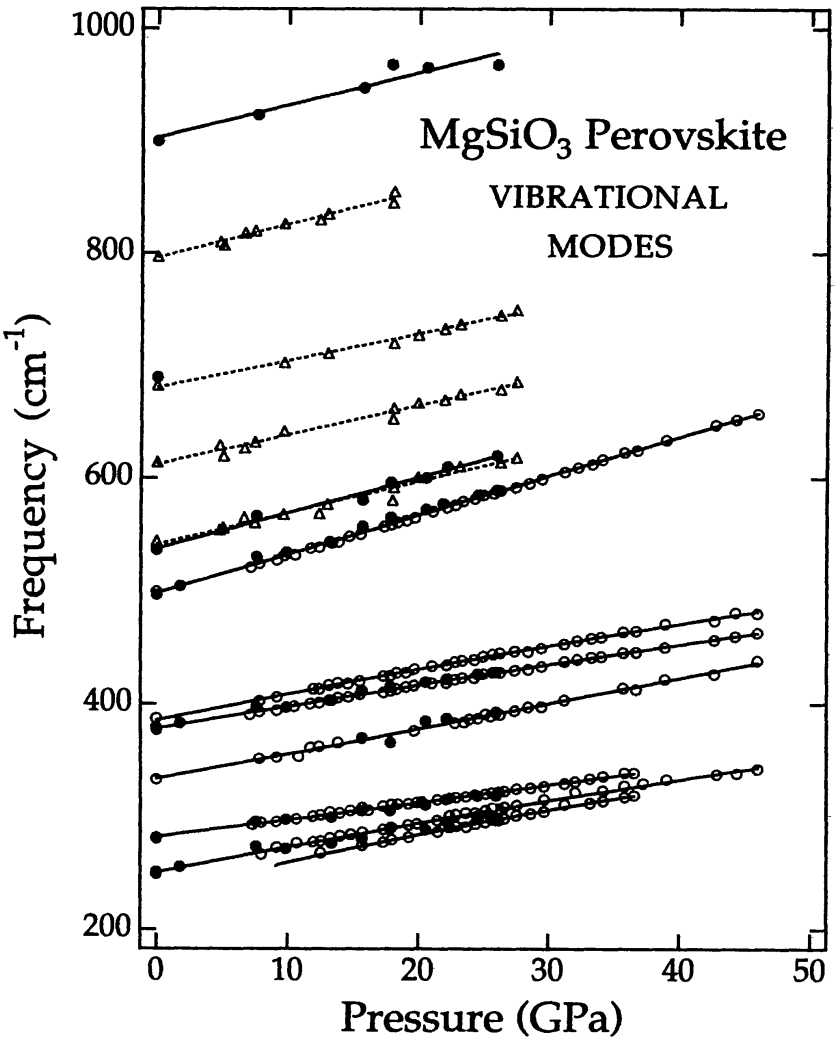

Figure 13 Pressure dependence of the vibrational frequencies for $MgSiO_3$ perovskite (room temperature). Raman modes: ●, Hemley et al (1989); ○, Chopelas & Boehler (1992). Infrared modes: △, Williams et al (1987). The solid and dashed lines are least-squares fits to the pressure shifts for the Raman and infrared modes, respectively.

sum includes in principle all vibrational modes i (see Hemley et al 1989). The sum over the available data gives $\langle\gamma_i\rangle = 1.80$–$2.03$ ($q = 0-2$) at 300 K and $\langle\gamma_i\rangle = 1.67$–$1.87$ at high temperature which is close to previous results (Hemley et al 1989, Williams et al 1989). Despite the wealth of new information on the vibrational properties of this material at high pressures, accurate calculation of γ_{th} from spectroscopic data is still problematic because the pressure shifts for most of the modes have not been measured and there may be inadequate sampling of the vibrational density of states.

An additional application of vibrational spectroscopic measurements of silicate perovskite has been their use in characterizing the materials at low

pressures. This has been particularly important because of the ease with which samples transform to glassy phases at low pressures (e.g. zero pressure) when subjected to heating, laser illumination, and grinding or polishing (Hemley et al 1989, Yeganeh-Haeri et al 1989b, Wolf et al 1990). The glass phase, which is formed prior to crystallization of enstatite (Knittle & Jeanloz 1987b), is readily observed by vibrational spectroscopy and may not be apparent in standard x-ray diffraction or x-ray spectroscopic measurements. There is evidence that the extent of amorphization depends on both sample history and the method of preparation. Amorphization also complicates high-temperature Raman measurements on silicate perovskites, which are important for studying possible temperature-induced soft-mode behavior. Preliminary Raman spectra as a function of temperature up to the point of vitrification at zero pressure have been reported for $MgSiO_3$ (Wolf et al 1990, Durben & Wolf 1991). The frequencies ν decrease with temperature, but no anomalous soft-mode behavior (defined as $\nu \rightarrow 0$) has yet been observed. Because of amorphization, such measurements need to be performed at high pressure, within the stability field of the perovskite.

HIGH-TEMPERATURE PHASE TRANSITIONS

The question of high-temperature phase transitions in distorted perovskites is closely related to the vibrational dynamics as observed in Raman spectroscopy because many of the possible transitions would involve soft-mode behavior with some mode frequencies vanishing (or becoming small) at the phase transition. Continuous transitions in perovskite, if they did occur in the Earth, would be particularly important if they involve soft Raman modes because they would then lead to elastic or acoustic anomalies in shear moduli at the phase transition. Thus, for example, a soft-mode transition from an orthorhombic phase to a tetragonal phase would involve probable softening of c_{11}–c_{12}, and transition from the orthorhombic phase to a monoclinic phase would involve softening of a shear mode (e.g. c_{66}). Also, the average shear modulus could show non-monotonic behavior as a function of pressure and/or temperature.

There are a number of possible phase transitions in perovskite with increasing temperature that involve loss of the various octahedral tilts, culminating with the cubic structure, possibly at temperatures above the melting point. Aleksandrov (1976, 1978) discussed some possibilities for phase transitions from *Pbnm*, but his analysis assumed that symmetry will always be increased with increasing temperature—which is not necessarily the case. The subset of transitions he considered that refer to *Pbnm*

is shown by the square blocks in Figure 14. The structures in the circles are for possible intermediate phases which tend to have lower symmetry but lead from one tilt system to another in cases where Aleksandrov considered only discontinuous phase transitions possible. Thus if $(Mg,Fe)SiO_3$ does transform at high temperatures to another distorted perovskite [$q^-a^-c^+$ using Glazer's (1975) notation], it is most likely to transform to tetragonal $D_{4h}^5(00c^+)$, orthorhombic $D_{2h}^{28}(a^-a^-0)$, monoclinic $C_{2h}^2(a^-b^-c^+)$, or to orthorhombic $D_{2h}^{17}(0a^-c^+)$.

Glazer's + and − type tilts can be related to M_2 and R_{25} instabilities. In other words, the atomic displacements are modulated by $\cos[-q\cdot r]$, where q is given by $(0.5,0.5,0)$ (in units of $2\pi/a$) for the M-point and $(0.5,0.5,0.5)$ for the R-point and r is the lattice vector (relative to the cubic lattice). Figure 1 shows the M_2- and R_{25}-type rotations. There is one three-dimensionally degenerate R-point in the cubic Brillouin zone and there are three distinct M-points. Thus the rigid tilts in perovskite can be represented

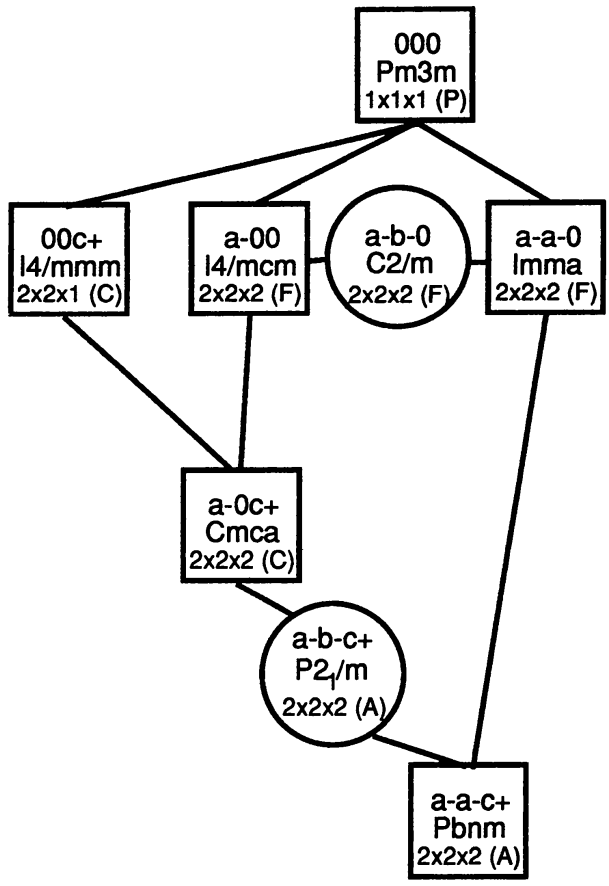

Figure 14 Possible structural phase transitions in perovskite from cubic *Pm3m* to lower symmetry perovskite structures.

as coordinates in a six-dimensional space, only a subset of which can be described by Glazer's notation. The R_{25} and M_2 modes are folded into the zone center in *Pbnm* and become Raman-active modes. One or more of these modes might be expected to display soft-mode behavior near a continuous high-temperature phase transition. However, many of the Raman modes are not observed since they are too weak (Williams et al 1987, Hemley et al 1989, Chopelas & Boehler 1992), and no such soft-mode behavior has yet been observed in $MgSiO_3$ perovskite.

It is crucial to investigate which modes in *Pbnm* perovskite correspond to the R_{25} and M_2 modes in cubic perovskite and whether these modes are expected to go soft at various phase transitions. A symmetry analysis of *Pbnm* perovskite was performed using the method of Boyer (1974). By examining the symmetry modes, we find that only A_g symmetry modes are compatible with tilt distortions that can lead to continuous phase transitions at high temperatures. There are two A_g modes compatible with M_2 symmetry and two A_g modes compatible with R_{25} symmetry. Thus lack of soft-mode behavior in the A_g modes is sufficient to rule out soft-mode behavior in a *Pbnm* perovskite. A transition to *Imma* would likely be a soft-mode transition. A soft-mode transition to *I4/mmm* would require two R_{25}-type modes going soft simultaneously. A direct transition to *Cmcm* would be first-order, though *Cmcm* could be reached continuously through a monoclinic $P2_1/m$ structure. The latter path also would not involve soft-mode behavior. In general, a second-order, continuous phase transition does not require soft-mode behavior. An example is the transitions in $La_{2-x}Ba_xCuO_4$ (Pickett et al 1991). The phase transition could have order-disorder character, where above the phase transition temperature T_c there would be uncorrelated local tilts which become correlated as temperature decreases until a phase transition occurs, at which point the tilts are all in phase. Order-disorder transitions can couple with elastic constants and cause elastic anomalies as well as soft-mode transitions.

A variety of calculations have considered the relative stability of cubic and orthorhombic $MgSiO_3$. Wolf & Bukowinski (1987) and Bukowinski & Wolf (1988) predicted that the series of transitions orthorhombic → tetragonal → cubic in $MgSiO_3$ occurs in the mantle with increasing temperature. These calculations, however, significantly underestimate the distortion of the orthorhombic form in comparison to experiment (Figure 3), and hence its stability relative to cubic. Also, the phase transition temperature was not calculated directly but was estimated by extrapolating the results of quasi-harmonic calculations assuming critical behavior in the tilts as functions of temperature; however, quasi-harmonic calculations do not include the fluctuations that cause critical behavior. It is necessary to perform anharmonic calculations with interatomic potentials that more

accurately reproduce the room P-T structure (e.g. Hemley et al 1987). Using the PIB model Cohen (1987) found that the energy difference (expressed as temperature) between cubic and orthorhombic $MgSiO_3$ rose rapidly by 60 K GPa^{-1}. Though the energy difference is 6700 K at 100 GPa, the results are sensitive to small changes in the interatomic potentials. Matsui & Price (1991), using their empirical rigid ion potential, predict that the transition occurs just below their theoretically predicted T_m, which is very high (Figure 11). They found a continuous transition from orthorhombic to cubic, which is not allowed in a soft-mode transition, and indicates order-disorder character.

Wang et al (1990, 1992) have interpreted the extensive twinning observed in electron microscopic studies of quenched samples of $(Mg,Fe)SiO_3$ perovskite as evidence for a structural transformation at high P and T. The observation of twins (Wang et al 1990) does not in itself indicate that the twins are formed by cooling through a phase transition, but the more recent observations (Wang et al 1992) that crystals quenched from above 1870 K at 26 GPa contain more twins than samples annealed below 1570 K is suggestive of a phase transition. They suggest that the transition is to the tetragonal $P4/mbm$ ($00c^+$) or $I4/mcm$ (a^-00) structures. Wang et al (1992) suggest that the kink observed in the melting curve of perovskite by Knittle & Jeanloz (1989a) arises from the intersection with the same perovskite structural phase transition they observe at lower pressures (Figure 11). If correct, this proposal would imply that seismic velocity (or density) anomalies arising from this transition should occur at a depth corresponding to ~ 50 GPa in the lower mantle. A transition from orthorhombic to tetragonal should correspond to a softening of the shear modulus $c_{11}-c_{12}$ at the transition. Although these results are quite compelling, the interpretations are complicated by sample decomposition effects under the electron beam, the possibility that samples annealed at higher temperatures have coarser twins (and thus are easier to observe), greater equilibrium density of twins at higher temperature, and compositional changes in the various runs. Wang et al (1992) also studied analogue perovskites $CaTiO_3$, $CaGeO_3$, $MnGeO_3$, $LaGaO_3$, and $SmAlO_3$ which have $Pbnm$ structure at ambient conditions and observed similar twinning textures for samples quenched from below and above a phase transition. Although this provides further support for the proposal for a phase transition in $(Mg,Fe)SiO_3$, it should be pointed out that intermediate plagioclase feldspars contain ubiquitous polysynthetic twins which are not the result of any phase transitions.

Evidence for another phase transition has been reported by Wang et al (1991a) on the basis of direct x-ray diffraction measurements of $MgSiO_3$ perovskite as a function of temperature to 1200 K at 7.1 GPa. On the basis

of shifts of the *113* diffraction peak, a temperature-induced phase transition to another orthorhombic structure at 600 K was proposed (see Figure 7). They concluded that the thermal expansion coefficient of the perovskite is significantly smaller than the previous measurements and further that the structure of the *Pbnm* orthorhombic perovskite may not be representative of the mineral in the Earth. However, the magnitude of the volume discontinuity initially observed at the proposed phase transition is reported to be smaller in subsequent studies (Weidner et al 1991) and may not be statistically significant. Other diffraction experiments carried out in this pressure range also do not support the results of the Wang et al study (Mao et al 1991, Y. Fei, personal communication). The discrepancy could be associated with texturing effects in the former samples, which can introduce errors in the determination of peak positions in powder diffraction patterns. In view of the complications arising from studies of perovskite at lower pressures (e.g. amorphization), the issue also reinforces the need for careful measurements on the material within its stability field ($P > 23$ GPa).

The observation of ferroelectricity in perovskites has given rise to the suggestion that silicate perovskites might undergo similar ferroelectric transitions, perhaps at lower mantle conditions (Litov & Anderson 1978, Anderson 1988). The charge distribution of the end-member $MgSiO_3$ is largely ionic and does not reveal the type of Ti *d*-orbital hybridization found for $BaTiO_3$ that may be responsible for ferroelectric behavior in the latter material (Cohen & Krakauer 1990). This does not rule out possible ferroelectric-type behavior on substitution of other cations in silicate perovskite.

TRANSPORT PROPERTIES

Other important physical properties are the transport properties of silicate perovskite, such as electrical conductivity, thermal conductivity, and rheology. These properties are needed for modeling convection, thermal history, and the Earth's magnetic field, but they are very difficult to study because of the instability of perovskite under ambient conditions and technical difficulties associated with measurement of transport properties under extreme conditions of temperature and pressure. Despite these problems, significant progress has been made, and the first direct measurements have been reported.

The electrical conductivity of mantle phases strongly controls the strength of the magnetic field at the Earth's surface. Measurements of the electrical conductivity of silicate perovskite at high P and T has therefore been of great interest. These challenging experiments have been at the limit

of high-pressure techniques, and the results are accordingly controversial. Li & Jeanloz (1987, 1990) reported measurements of electrical conductivity of $(Mg,Fe)SiO_3$ at high P and T using laser-heated diamond-cell techniques. Their results indicated that the conductivity of the Mg end-member is several orders of magnitude lower than geophysical observations for the lower mantle (Li & Jeanloz 1987). Subsequent measurements indicated a large effect from Fe, but the conductivity of $(Mg_{0.9}Fe_{0.1})SiO_3$ perovskite is still lower than geophysical data for the lower mantle (Li & Jeanloz 1990, Li et al 1991). Peyronneau & Poirier (1989) measured the conductivity of both perovskite and perovskite-magnesiowüstite assemblages at high pressures, but using resistance heating (to 673 K); extrapolating these results to lower-mantle temperatures gives a value for the conductivity in good agreement with geomagnetic models. The measurements are extremely sensitive to contamination by water (Li & Jeanloz 1991, Poirier & Peyronneau 1991). Both laboratories now obtain agreement for the conductivity of high iron-content samples containing 20% Fe/(Fe+Mg), which consist of perovskite and magnesiowüstite mixtures, although there is still a discrepancy for iron compositions. These results are not consistent with the dominant conduction mechanism for perovskite being ionic (O'Keeffe & Bovin 1979, Poirier et al 1983, Kapusta & Guillope 1988, Wall & Price 1989), although very recent theoretical calculations predict that ionic conductivity could be important very close to melting (Matsui & Price 1991). It should be noted that the evidence for ionic conductivity in fluoride analogues (O'Keeffe et al 1979) has been attributed to surface effects (Andersen et al 1985). Finally, these experiments also indicate that the conductivity of (Mg,Fe)O is significantly higher than that of $(Mg,Fe)SiO_3$ perovskite, and that this mineral may dominate the conductivity of the lower mantle (Li & Jeanloz 1990, Wood & Nell 1991).

Little is known about thermal conductivity, κ, at high pressures and temperatures except for model extrapolations from low-pressure measurements (Kieffer 1976, Roufosse & Jeanloz 1983, Brown 1986). Until recently, no measurements were available for silicate perovskite. Osako & Ito (1991) measured the thermal diffusivity $a = C_p\rho\kappa$ of a large polycrystalline sample of $MgSiO_3$ between 160 and 340 K and fit the results to $1/a = A + BT$ where $A = (-6.2 \pm 1.4) \times 10^4$ m^{-2} s and $B = (2.15 \pm 0.05) \times 10^3$ m^2 s K^{-1}. They obtain $\kappa = 5.1$ W m^{-1} K^{-1} under ambient conditions which is similar to other silicates. Extrapolating to lower mantle conditions they estimated $\kappa = 3.0$ W m^{-1} K^{-1} at 670 km depth at 1900 K and 12 W m^{-1} K^{-1} at the top of the D'' layer at 2500 K. They suggest that the thermal conductivity would be high enough to prevent the D'' layer at the base of the mantle from being a thermal boundary layer.

An understanding of the rheological properties of silicate perovskite at high pressures and temperatures is crucial for detailed modeling of convection in the Earth. This has been addressed in several theoretical studies of ion migration in $MgSiO_3$ perovskite (Wall et al 1986, Price et al 1989, Miyamoto 1988). This is a very difficult problem experimentally because laboratory time scales are many orders of magnitude shorter than flow time scales in the Earth. Nevertheless, measurements of the plasticity of silicate perovskites are beginning. The plasticity of single crystals of $MgSiO_3$ perovskite has been studied at 300 K and found to be higher than that of olivine and enstatite (Karato et al 1990). Estimates of the shear strength of $(Mg,Fe)SiO_3$ and magnesiowüstite have been obtained from measurements and analyses of the pressure distribution supported by polycrystalline samples in the diamond-cell (Meade & Jeanloz 1990). The results indicated a maximum shear stress of approximately 7 GPa under lower-mantle pressures and room temperature, compared with 8.5 GPa for $(Mg,Fe)_2SiO_4$ spinel, and the authors speculated that the lower mantle may be more ductile than the transition zone. Ito & Sato (1991) argue that the absence of seismicity below 700 km arises from superplasticity associated with the fine-grain texture of perovskite and magnesiowüstite assemblages in the lower mantle.

Under the high temperatures and low strain rates of the lower mantle, yield stress itself is not a pertinent quantity, rather the viscosity or strain rate versus stress is important. The latter are essentially unknown for minerals under lower mantle conditions and in fact may be governed by magnesiowüstite rather than perovskite. In order to address the problem of temperature dependence of the rheology of perovskite, Beauchesne & Poirier (1989, 1990) have studied high-temperature creep in $BaTiO_3$, $KTaO_3$, $KNbO_3$, $RbCaF_3$, and $KZnF_3$ perovskites and found that each perovskite behaved qualitatively differently; thus it was impossible to draw general conclusions about perovskite deformation at high temperatures. The results were fit to the form: $\dot{\varepsilon} = A\sigma^n \exp(-Q/RT)$, where $\dot{\varepsilon}$ is the strain rate, σ is the shear stress, R is the gas constant, T is temperature, Q is the activation energy, and n is the stress exponent. They found that n varies from 1 to 3.7, ln A varies from -11 to -62 (σ is in Pa), and Q varies from 116 to 469 kJ/mole in the three oxide perovskites they studied. This would imply a drop in strength (or increase in strain rates) of many orders of magnitude between room temperature and mantle temperatures. In summary, little remains known about deformation of perovskite under mantle conditions, but progress has been made at low temperatures and high pressures and, on other perovskites, at high temperatures and zero pressure.

DISCUSSION

The increasing number of measurements of the physical and chemical properties of silicate perovskites has provided an essential database for unifying mineralogical, geochemical, and seismological models of the Earth's lower mantle (Silver et al 1988, Anderson 1989). There is now a fair amount of agreement concerning the structural properties and equation of state, including the bulk modulus and thermal expansivity. The measurements provide new insight into interpretation of the 670-km discontinuity, seismologically determined density profiles, the D'' region, and the core-mantle boundary. However, it must also be said that a complete and accurate description of the physical properties of these phases at mantle conditions is not yet in hand, as is evident from the number of controversies that need to be resolved. Thus, one of the central questions in solid-earth geophysics—the composition of the lower mantle, and whether it is chemically distinct and convecting separately from that of the upper mantle—continues to be a matter of active debate. A detailed review of this topic, including mineral physics data for both silicate perovskites and oxide phases and analyses of different seismological models is presented by Bina & Hemley (to be published). Here we point out key constraints from measurements on silicate perovskites.

The phase equilibrium study of Ito & Takahashi (1989) has reaffirmed the coincidence of $(Mg,Fe)_2SiO_4$ silicate spinel to perovskite plus magnesiowüstite transition with the 670-km discontinuity, including the sharpness of the transition, in agreement with earlier diamond-cell studies. They argue that the 670-km discontinuity is therefore compatible with the occurrence of an isochemical transformation in this system and with a homogeneous peridotitic composition for the upper and lower mantle. In principle, the P-T slopes of the perovskite-forming reactions provide another constraint, but the measured values are not sufficiently negative, or well enough determined experimentally, to rule out mixing of the upper and lower mantle (Ito et al 1990). Currently, the most reliable constraint on the chemical composition is provided by density measurements on candidate upper-mantle compositions at lower-mantle pressures. Jeanloz & Knittle (1989) have calculated densities for perovskite and magnesiowüstite at lower mantle conditions from equation of state models determined in part from experimental data. They conclude that for a range of predicted geotherms upper mantle compositions are incompatible with seismic data (Dziewonski & Anderson 1981) in the lower mantle; specifically, an iron enrichment (bulk iron component of 15%) is required, with the intrinsic density of the lower mantle 2.6% (and possibly up to 5%) higher than the upper mantle. Their results are dependent on as-yet un-

measured parameters at high P-T conditions (Chopelas & Boehler 1989, Bina & Silver 1990, Bukowinski & Wolf 1990). The high-P-T x-ray diffraction results (Mao et al 1991) support the equations of state used in this analysis but indicate there is a significant decrease in thermal expansion that is not included in these calculations. Hemley et al (1992) have shown that including this effect decreases the need for iron enrichment at the top of the lower mantle (with no thermal boundary layer), although silica enrichment is then required (Liu 1979, Bass & Anderson 1984, Kuskov & Panferov 1991). Further analysis of the density profile for the entire lower mantle, where the density is better constrained seismologically, as well as for the seismic parameter, is given by Bina & Hemley (1992). A change in chemical composition should give rise to a thermal boundary layer, and two separately convecting systems in the upper and lower mantle. If so, iron enrichment then becomes a plausible means by which to offset the effect of higher temperatures (thermal expansion) in order to be consistent with the seismic density profiles (Jeanloz & Knittle 1989). A compositional boundary, if present, may not occur at the identical depth as the phase transition to perovskite-bearing assemblages (Jeanloz 1991).

As described above, transitions to higher symmetry forms have been predicted to occur with increasing temperature in $(Mg,Fe)SiO_3$ perovskite, and these transitions could complicate such inferences for the composition of the lower mantle (Wang et al 1992). There is currently no direct experimental evidence for these transitions, although similar transitions are documented for isostructural perovskite materials. If perovskite is cubic under lower mantle P-T conditions, its bulk modulus is expected to increase as a result of the loss of degrees of freedom for compression. Theoretical calculations indicate that the bulk modulus could increase by $\sim 5\%$ on going from orthorhombic to cubic (Cohen et al 1989). Such antiferroelastic transitions, which may be soft-mode driven, may give rise to unusual shear softening as the transitions are approached. Yeganeh-Haeri et al (1989a) have proposed that transitions of this type may be responsible for the high values of $d\ln V_s/d\ln V_p$ (≈ 2–3) observed in studies of lateral heterogeneity in the lower mantle (e.g. Dziewonski & Woodhouse 1987). Recent calculations show, however, that such behavior can arise from the effect of temperature on the shear modulus relative to the bulk modulus at high P and T in simple materials such as MgO (Isaak et al 1990, 1992; Agnon & Bukowinski 1990; Anderson et al 1992), which do not exhibit these transitions.

The $CaSiO_3$ perovskite exists in the lower mantle as a major separate phase with an abundance subordinate only to ferromagnesian silicate perovskite and, most probably, to magnesiowüstite. The weight percentage of $CaSiO_3$ perovskite is 6.2% in the pyrolite model, 7.0% in a recent model

based on solar abundances, and 12% in the piclogite model. Since $CaSiO_3$ also has a higher bulk modulus than $(Mg,Fe)SiO_3$ (by $\sim 3\%$) (Mao et al 1991), an appreciable enrichment of Ca in the lower mantle could contribute to increasing K_S. Such a comparison could be used to bound the Ca abundance in the lower mantle, since sufficient constraints cannot be obtained from the density alone (see Mao et al 1989a). These results will also depend on the thermal expansivity of the calcium perovskite at mantle conditions, which has not been measured. Ita & Stixrude (1991) have suggested that the $CaSiO_3$ perovskite transition could be responsible for seismic structure near 520 km (i.e. in the transition zone) (Shearer 1990). Recent studies have indicated that partitioning of rare earth elements in $CaSiO_3$ perovskite is significantly higher than that in $(Mg,Fe)SiO_3$ perovskite (Ito & Takahashi 1987b; Kato et al 1988a,b). If so, cubic $CaSiO_3$ perovskite could represent a large reservoir of rare earth elements in the mantle. However, the effects of disequilibrium in such experiments have been questioned (Walker & Agee 1989).

OUTLOOK

Progress on the study of silicate perovskite during the past few years may be characterized as moving from the study of analogue materials, to studies carried out at ambient (room) conditions, and finally to the in situ study at high pressures. In situ studies of silicate perovskites under combined high pressure and high temperatures are in their infancy (Mao et al 1991), and few have yet been performed under lower mantle P-T conditions. Future work will likely be characterized by in situ measurements under these extreme conditions, including petrologic studies of whole rock samples at deep mantle conditions (e.g. O'Neill & Jeanloz 1990). As in the past, accurate ultrahigh-P-T measurements will require continued development of both high-pressure technology and analytical techniques. With these developments it is probable that further progress will also be made in the study of transport properties, which could provide important additional constraints on mantle mineralogy. These may be controlled by the defect chemistry of silicate perovskites at high temperatures and pressures, about which little is currently known.

If our current understanding of the phase equilibria under lower mantle conditions is correct, then the study of the properties of $(Mg,Fe)SiO_3$ and $CaSiO_3$ perovskite, along with magnesiowüstite and stishovite, should fully describe the physical properties of the lower mantle. It is important to recognize that our understanding of the deep earth may be biased by the properties of those materials that can be quenched to low (ambient) conditions or otherwise easily studied in the laboratory. Evidence for new

nonquenchable aluminous, calcic, and magnesium silicate phases which are stable under lower mantle conditions has been reported (Guyot et al 1989, Ito 1989, Kubicki & Hemley 1989) and others have been predicted (e.g. Finger & Hazen 1991), and new classes of chemical reactions occurring at deep mantle conditions are indeed likely (e.g. Knittle & Jeanloz 1989b, 1991a). It is likely to take many years to fully describe the elastic, rheological, and transport properties of these materials and the deep rocks that they constitute. In so doing, new insights into properties of silicates and oxides will be gained, new high-*P-T* technology and computational techniques will be developed, and a better understanding of the Earth and its history will be achieved.

ACKNOWLEDGMENTS

We are grateful to the following for their help in the preparation of this review: Y. Fei, L. W. Finger, R. M. Hazen, E. Ito, R. Jeanloz, H. K. Mao, C. E. Meade, A. Navrotsky, C. T. Prewitt, G. D. Price, L. Stixrude, Y. Wang, Q. Williams, and G. H. Wolf. Computations were performed on the Cray 2 at the NCSA under the auspices of the NSF. NSF grants EAR-8904080, EAR-8920239, and EAR-8916754 supported this work.

Literature Cited

Agnon, A., Bukowinski, M. S. T. 1990. δ_s at high pressure and $d\ln V_s/d\ln V_p$ in the lower mantle. *Geophys. Res. Lett.* 17: 1149–52

Aleksandrov, K. S. 1976. The sequences of structural phase transitions in perovskites. *Ferroelectrics* 14: 801–5

Aleksandrov, K. S. 1978. Mechanisms of the ferroelectric and structural phase transitions, structural distortions in perovskites. *Ferroelectrics* 20: 61–67

Andersen, N. H., Kjems, J. K., Hayes, W. 1985. Ionic conductivity of the perovskites $NaMgF_3$, $KMgF_3$, and $KZnF_3$ at high temperatures. *Solid State Ionics* 17: 143–45

Anderson. D. L. 1989. *Theory of the Earth.* Boston: Blackwell. 366 pp.

Anderson, O. L. 1988. A ferroelectric transition in the lower mantle? *Eos Trans. Am. Geophys. Union* 69: 1451 (Abstr.)

Anderson, O. L., Chopelas, A., Boehler, R. 1990. Thermal expansivity versus pressure at constant temperature: A re-examination. *Geophys. Res. Lett.* 17: 685–88

Anderson, O. L., Isaak, D., Oda, H. 1992. High-temperature elastic constant data on minerals relevant to geophysics. *Rev. Geophys.* In press

Andrault, D., Poirier, J. P. 1991. Evolution of the distortion of perovskites under pressure: an EXAFS study of $BaZrO_3$, $SrZrO_3$, and $CaGeO_3$. *Phys. Chem. Miner.* 18: 91–105

Bass, J. D., Anderson, D. L. 1984. Composition of the upper mantle: geophysical tests of two petrological models. *Geophys. Res. Lett.* 11: 237–40

Bassett, W. A., Weathers, M. S., Huang, E., Onomichi, M. 1988. Melting curve of $Mg_{0.88}Fe_{0.12}SiO_3$ up to 700 kbar. *Eos Trans. Am. Geophys. Union* 69: 1451 (Abstr.)

Beauchesne, S., Poirier, J. P. 1989. Creep of barium titanate perovskite: a contribution to a systematic approach to the viscosity of the lower mantle. *Phys. Earth Planet. Inter.* 55: 187–99

Beauchesne, S., Poirier, J. P. 1990. In search of a systematics for the viscosity of perovskites: creep of potassium tantalate and niobate. *Phys. Earth Planet. Inter.* 61: 182–98

Bell, P. M., Yagi, T., Mao, H. K. 1979. Iron-magnesium distribution coefficients between spinel $[(Mg,Fe)_2SiO_4]$, magnesiowüstite $[(Mg,Fe)O]$, and perovskite $[(Mg,Fe)SiO_3]$. *Carnegie Inst. Washington Yearb.* 78: 618–21

Bina, C. R., Helffrich, G. R. 1992. Cal-

culation of elastic properties from thermodynamic equation of state principles. *Annu. Rev. Earth Planet. Sci.* 20: 527–52

Bina, C. R., Silver, P. 1990. Constraints on lower mantle composition and temperature from density and bulk sound velocity profiles. *Geophys. Res. Lett.* 17: 1153–56

Boehler, R., Chopelas, A. 1991. A new approach to laser heating in high pressure mineral physics. *Geophys. Res. Lett.* 18: 1147–50

Boehler, R., Chopelas, A. 1992. Phase transitions in a 500 kbar–3000 K gas apparatus. See Syono & Manghnani 1992. In press

Boyer, L. L. 1974. Computerized group theory for lattice dynamical problems. *J. Comput. Physics* 16: 167–85

Brown, J. M. 1986. Interpretation of the *D″* zone at the base of the mantle: dependence on assumed values of thermal conductivity. *Geophys. Res. Lett.* 13: 1509–12

Bukowinski, M. S. T., Wolf, G. H. 1988. Equation of state and possible critical phase transitions in $MgSiO_3$ perovskite at lower-mantle conditions. In *Advances in Physical Geochemistry, Vol. 7 Structural and Magnetic Phase Transitions*, ed. S. Ghose, J. M. D. Coey, E. Salje, pp. 91–112. New York: Springer-Verlag

Bukowinski, M. S. T., Wolf, G. H. 1990. Thermodynamically consistent decompression: implications for lower mantle composition. *J. Geophys. Res.* 95: 12,583–93

Chen, L. C., Mao, H. K., Hemley, R. J. 1989. Compression and polymorphism of $CaSiO_3$ at high pressures and temperatures. *Annu. Rep. Dir. Geophys. Lab.* 1988–1989: 94–98

Chopelas, A., Boehler, R. 1989. Thermal expansion at very high pressure, systematics, and a case for a chemically homogeneous mantle. *Geophys. Res. Lett.* 16: 1347–50

Chopelas, A., Boehler, R. 1992. Raman spectroscopy of high pressure $MgSiO_3$ phases synthesized in a CO_2 laser heated diamond anvil cell: perovskite and clinopyroxene. See Syono & Manghnani 1992. In press

Choudhury, N., Chaplot, S. L., Rao, K. R., Ghose, S. 1988. Lattice dynamics of $MgSiO_3$ perovskite. *Pramana J. Phys.* 30: 423–28

Christensen, U. R., Yuen, D. A. 1984. The interaction of a subducting lithosphere with a chemical or phase boundary. *J. Geophys. Res.* 89: 4389–4402

Cohen, R. E. 1987. Elasticity and equation of state of $MgSiO_3$ perovskite. *Geophys. Res. Lett.* 14: 1053–56

Cohen, R. E., Boyer, L. L., Mehl, M. J., Pickett, W. E., Krakauer, H. 1989. Electronic structure and total energy calculations for oxide perovskites and superconductors. See Navrotsky & Weidner 1989, pp. 55–66

Cohen, R. E., Krakauer, H. 1990. Lattice dynamics and origin of ferroelectricity in $BaTiO_3$: Linearized-augmented-plane-wave total-energy calculations. *Phys. Rev. B* 42: 6416–23

Durben, D. J., Wolf, G. H. 1991. Thermally-induced vitrification and internal stress in magnesium silicate ($MgSiO_3$) perovskite. *Eos Trans. Am. Geophys. Union* 72(44): 464 (Abstr.)

Dziewonski, A. M., Anderson, D. L. 1981. Preliminary reference earth model. *Phys. Earth Planet. Inter.* 25: 297–356

Dziewonski, A. M., Woodhouse, J. H. 1987. Global images of the Earth's interior. *Science* 236: 37–48

Fei, Y., Mao, H. K., Hemley, R. J., Shu, J. 1991a. Simultaneous high-P-T diffraction measurements of $(Fe,Mg)SiO_3$-perovskite and (Fe,Mg)O magnesiowüstite: implications for lower mantle composition. *Annu. Rep. Dir. Geophys. Lab.* 1990–1991: 107–14

Fei, Y., Mao, H. K., Mysen, B. O. 1991b. Experimental determination of element partitioning and calculation of phase relations in the MgO-FeO-SiO_2 system at high pressure and high temperature. *J. Geophys. Res.* 96: 2157–69

Finger, L. W., Hazen, R. M. 1991. Crystal chemistry of six-coordinated silicon: a key to understanding the Earth's deep interior. *Acta Crystallogr.* B47: 561–80

Fitz Gerald, J. D., Ringwood, A. E. 1991. High pressure rhombohedral perovskite phase $Ca_2AlSiO_{5.5}$. *Phys. Chem. Miner.* 18: 40–46

Glazer, A. M. 1972. The classification of tilted octahedra in perovskites. *Acta Crystallogr. Ser. B* 28: 3384–92

Glazer, A. M. 1975. Simple ways of determining perovskite structures. *Acta Crystallogr. Ser. A* 31: 756–62

Guyot, F., Madon, M., Peyronneau, J., Poirier, J. P. 1989. X-ray microanalysis of high-pressure/high-temperature phases synthesized from natural olivine in a diamond-anvil cell. *Earth Planet. Sci. Lett.* 90: 52–64

Hazen, R. M. 1988. Perovskites. *Scientific American*, June 1988: 74–81

Heinz, D. L. 1991. Split decision on the mantle. *Nature* 351: 346–47

Heinz, D. L., Jeanloz, R. 1987. Measurement of the melting curve of $Mg_{0.1}Fe_{0.9}SiO_3$ perovskite at lower mantle conditions and its geophysical implications. *J. Geophys. Res.* 92: 11,437–44

Hemley, R. J. 1991. Spectroscopic models for thermodynamic properties of minerals at high pressures and temperatures. *EOS Trans. Am. Geophys. Union* 72(12): 282 (Abstr.)

Hemley, R. J., Cohen, R. E., Yeganeh-Haeri, A., Mao, H. K., Weidner, D. J., Ito, E. 1989. Raman spectroscopy and lattice dynamics of $MgSiO_3$ perovskite at high pressure. See Navrotsky & Weidner 1989, pp. 35–44

Hemley, R. J., Jackson, M. D., Gordon, R. G. 1985. Lattice dynamics and equations of state of high-pressure mineral phases studied with electron-gas theory. *Eos Trans. Am. Geophys. Union* 66: 357 (Abstr.)

Hemley, R. J., Jackson, M. D., Gordon, R. G. 1987. Theoretical study of the structure, lattice dynamics, and equations of state of perovskite-type $MgSiO_3$ and $CaSiO_3$. *Phys. Chem. Miner.* 14: 2–12

Hemley, R. J., Kubicki, J. D. 1991. Deep mantle melting. *Nature* 349: 283–84

Hemley, R. J., Stixrude, L., Fei, Y., Mao, H. K. 1992. Constraints on lower mantle composition from *P-V-T* measurements of $(Fe,Mg)SiO_3$ perovskite and (Fe,Mg)O. See Syono & Manghnani 1992. In press

Hill, R. J., Jackson, I. 1990. The thermal expansion of $ScAlO_3$—a silicate perovskite analogue. *Phys. Chem. Miner.* 17: 89–96

Hirsch, L. M., Shankland, T. J. 1991. Point defects in $(Mg,Fe)SiO_3$ perovskite. *Geophys. Res. Lett.* 18: 1305–8

Hofmeister, A. M., Williams, Q., Jeanloz, R. 1987. Thermodynamic and elastic properties of $MgSiO_3$ perovskite from far-IR spectra at pressure. *Eos Trans. Am. Geophys. Union* 68: 1469 (Abstr.)

Horiuchi, H., Ito, E., Weidner, D. J. 1987. Perovskite-type $MgSiO_3$: single crystal x-ray diffraction study. *Am. Mineral.* 72: 357–60

Irifune, T., Ringwood, A. E. 1987a. Phase transformations in primitive morb and pyrolite compositions to 25 GPa and some geophysical implications. See Manghnani & Syono 1987, pp. 231–42

Irifune, T., Ringwood, A. E. 1987b. Phase transformations in a harzburgite composition to 26 GPa: implications for dynamical behaviour of the subducting slab. *Earth Planet. Sci. Lett.* 86: 365–76

Irifune, T., Susaki, J., Yagi, T., Sawamoto, H. 1989. Phase transformations in diopside $CaMgSi_2O_6$ at pressures up to 25 GPa. *Geophys. Res. Lett.* 16: 187–90

Isaak, D. G., Anderson, O. L., Cohen, R. E. 1992. The relationship between shear and compressional velocities at high pressures: reconciliation of seismic tomography and mineral physics. *Geophys. Res. Lett.* Submitted

Isaak, D. G., Cohen, R. E., Mehl, M. J. 1990. Calculated elastic and thermal properties of MgO at high pressures and temperatures. *J. Geophys. Res.* 95: 7055–67

Ita, J., Stixrude, L. 1991. Petrology, elasticity and composition of the mantle transition zone. *J. Geophys. Res.* In press

Ito, E. 1977. The absence of oxide mixture in high-pressure phases of Mg-silicates. *Geophys. Res. Lett.* 4: 72–74

Ito, E. 1984. Ultra-high pressure phase relations of the system $MgO-FeO-SiO_2$ and their geophysical implications. In *Materials Science of the Earth's Interior*, ed. I. Sunagawa, pp. 387–94. Tokyo: Terra Scientific

Ito, E. 1989. Stability relations of silicate perovskite under subsolidus conditions. See Navrotsky & Weidner 1989, pp. 27–32

Ito, E., Akaogi, M., Topor, L., Navrotsky, A. 1990. Negative pressure-temperature slopes for reactions forming $MgSiO_3$ perovskite from calorimetry. *Science* 249: 1275–78

Ito, E., Katsura, T. 1992. Melting of ferromagnesian silicates under the lower mantle conditions. See Syono & Manghnani 1992

Ito, E., Matsui, Y. 1978. Synthesis and crystal-chemical characterization of $MgSiO_3$ perovskite. *Earth Planet. Sci. Lett.* 38: 443–50

Ito, E., Matsui, Y. 1979. High-pressure transformations in silicates, germanates, and titanates with ABO_3 stoichiometry. *Phys. Chem. Miner.* 4: 265–73

Ito, E., Sato, H. 1991. Aseismicity in the lower mantle by superplasticity of the descending slab. *Nature* 351: 140–41

Ito, E., Takahashi, E. 1987a. Ultrahigh-pressure phase transformations and the constitution of the deep mantle. See Manghnani & Syono 1987, pp. 221–29

Ito, E., Takahashi, E. 1987b. Melting of peridotite at uppermost lower-mantle conditions. *Nature* 328: 514–16

Ito, E., Takahashi, E. 1989. Postspinel transformations in the system Mg_2SiO_4-Fe_2SiO_4 and some geophysical implications. *J. Geophys. Res.* 94: 10,637–46

Ito, E., Takahashi, E., Matsui, Y. 1984. The mineralogy and chemistry of the lower mantle: an implication of the ultrahigh-pressure phase relations in the system $MgO-FeO-SiO_2$. *Earth Planet. Sci. Lett.* 67: 238–48

Ito, E., Weidner, D. J. 1986. Crystal growth of $MgSiO_3$ perovskite. *Geophys. Res. Lett.* 13: 464–66

Ito, E., Yamada, H. 1982. Stability relations

of silicate spinels, ilmenites and perovskite. In *High Pressure Research in Geophysics*, ed. S. Akimoto, M. H. Manghnani, pp. 405–19. Tokyo: Academic

Jackson, I. 1983. Some geophysical constraints on the chemical composition of the Earth's lower mantle. *Earth Planet. Sci. Lett.* 62: 91–103

Jackson, W. E., Knittle, E., Brown, G. E., Jeanloz, R. 1987. Partitioning of Fe within high-pressure silicate perovskite: evidence for unusual geochemistry in the lower mantle. *Geophys. Res. Lett.* 14: 224–26

Jeanloz, R. 1990. Thermodynamics and evolution of the Earth's interior: high-pressure melting of silicate perovskite as an example. *Proc. Gibbs Symp., Yale Univ., May 15–17, 1989*. Am. Math. Soc., pp. 211–26

Jeanloz, R. 1991. Effects of phase transitions and possible compositional changes in the seismological structure near 650 km depth. *Geophys. Res. Lett.* 18: 1743–46

Jeanloz, R., Knittle, E. 1989. Density and composition of the lower mantle. *Philos. Trans. R. Soc. London Ser. A* 328: 377–89

Jeanloz, R., Morris, S. 1986. Temperature distribution in the crust and mantle. *Annu. Rev. Earth Planet. Sci.* 14: 377–415

Jeanloz, R., O'Neill, B., Pasternak, M. P., Taylor, R. D., Bohlen, S. R. 1991. Mössbauer spectroscopy of $Mg_{0.1}Fe_{0.9}SiO_3$ perovskite. *Eos Trans. Am. Geophys. Union* 72(44): 464 (Abstr.)

Jeanloz, R., Thompson, A. B. 1983. Phase transitions and mantle discontinuities. *Rev. Geophys. Space Phys.* 21: 51–74

Kanzaki, M., Stebbins, J. F., Xue, X. 1991. Characterization of quenched high pressure phases in the $CaSiO_3$ system by XRD and ^{29}Si NMR. *Geophys. Res. Lett.* 18: 463–66

Kapusta, B., Guillope, M. 1988. High ionic diffusivity in the perovskite $MgSiO_3$: a molecular-dynamics study. *Phil. Mag. A* 58: 809–16

Karato, S., Fujino, K., Ito, E. 1990. Plasticity of $MgSiO_3$ perovskite: the results of microhardness tests on single crystals. *Geophys. Res. Lett.* 17: 13–16

Kato, T., Kumazawa, M. 1985. Garnet phase of $MgSiO_3$ filling the pyroxene-ilmenite gap at very high temperature. *Nature* 316: 803–5

Kato, T., Ringwood, A. E., Irifune, T. 1988a. Experimental determination of element partitioning between silicate perovskites, garnets, and liquids: constraints on early differentiation of the mantle. *Earth Planet. Sci. Lett.* 89: 123–45

Kato, T., Ringwood, A. E., Irifune, T. 1988b. Constraints on element partitioning coefficients between $MgSiO_3$ perovskite and liquid determined by direct measurements. *Earth Planet. Sci. Lett.* 90: 65–68

Kieffer, S. W. 1976. Lattice thermal conductivity within the earth and considerations of a relationship between the pressure dependence of the thermal diffusivity and the volume dependence of the Grüneisen parameter. *J. Geophys. Res.* 81: 3025–30

Kim, Y.-H., Ming, L. C., Manghnani, M. H., Ko, J. 1991. Phase transformation studies on a synthetic hedenbergite up to 26 GPa at 1200°C. *Phys. Chem. Miner.* 17: 540–44

Kirkpatrick, R. J., Howell, D., Phillips, B. L., Cong, X.-D., Ito, E., Navrotsky, A. 1991. MAS NMR spectroscopic study of $Mg^{29}SiO_3$ with the perovskite structure. *Am. Mineral.* 76: 673–76

Knittle, E., Closman, C., Li, G., Wang, X., Bridges, F. G. 1991. New x-ray absorption measurements on the site distribution of iron in silicate perovskite. *Eos Trans. Am. Geophys. Union* 72(44): 464 (Abstr.)

Knittle, E., Jeanloz, R. 1987a. Synthesis and equation of state of $(Mg,Fe)SiO_3$ perovskite to over 100 gigapascals. *Science* 235: 668–70

Knittle, E., Jeanloz, R. 1987b. The activation energy of the back transformation of silicate perovskite to enstatite. See Manghnani & Syono 1987, pp. 243–50

Knittle, E., Jeanloz, R. 1989a. Melting curve of $(Mg,Fe)SiO_3$ perovskite to 96 GPa: evidence for a structural transition in lower mantle melts. *Geophys. Res. Lett.* 16: 421–24

Knittle, E., Jeanloz, R. 1989b. Simulating the core-mantle boundary: An experimental study of high-pressure reactions between silicates and liquid ion. *Geophys. Res. Lett.* 16: 609–12

Knittle, E., Jeanloz, R. 1991. Earth's core-mantle boundary: Results of experiments at high pressures and temperatures. *Science* 251: 1438–43

Knittle, E., Jeanloz, R., Smith, G. L. 1986. The thermal expansion of silicate perovskite and stratification of the Earth's mantle. *Nature* 319: 214–16

Kubicki, J. D., Hemley, R. J. 1989. Spectroscopic evidence for a new high-pressure magnesium silicate phase. *Annu. Rep. Dir. Geophys. Lab.* 1988–1989: 91–94

Kubicki, J. D., Hemley, R. J., Hofmeister, A. M. 1992. Raman and infrared study of pressure-induced structural changes in $MgSiO_3$, $CaMgSi_2O_6$, and $CaSiO_3$ glasses. *Am. Mineral.* In press

Kubicki, J. D., Lasaga, A. C. 1991. Molecular dynamics simulations of pressure

and temperature effects on $MgSiO_3$ and Mg_2SiO_4 melts and glasses. *Phys. Chem. Miner.* 17: 661–73

Kudoh, Y., Ito, E., Takeda, H. 1987. Effect of pressure on the crystal structure of perovskite-type $MgSiO_3$. *Phys. Chem. Miner.* 14: 350–54

Kudoh, Y., Prewitt, C. T., Finger, L. W., Darovskikh, A., Ito, E. 1990. Effect of iron on the crystal structure of $(Mg,Fe)SiO_3$ perovskite. *Geophys. Res. Lett.* 17: 1481–84

Kuskov, O. L., Panferov, A. B. 1991. Phase diagrams of the FeO-MgO-SiO_2 system and the structure of the mantle discontinuities. *Phys. Chem. Miner.* 17: 642–53

Leinenweber, K., Navrotsky, A. 1988. A transferable interatomic potential for crystalline phases in the system MgO-SiO_2. *Phys. Chem. Miner.* 15: 588–96

Li, X., Jeanloz, R. 1987. Electrical conductivity of $(Mg,Fe)SiO_3$ perovskite and a perovskite-dominated assemblage at lower mantle conditions. *Geophys. Res. Lett.* 14: 1075–78

Li, X., Jeanloz, R. 1990. Laboratory studies of the electrical conductivity of silicate perovskites at high pressures and temperatures. *J. Geophys. Res.* 95: 5067–78

Li, X., Jeanloz, R. 1991. Phases and electrical conductivity of a hydrous silicate assemblage at lower-mantle conditions. *Nature* 350: 332–34

Li, X., Ming, L.-C., Manghnani, M. H., Wang, Y., Jeanloz, R. 1991. High-pressure experimental studies of the electrical conductivity of $(Mg_{0.9}Fe_{0.1})SiO_3$ perovskite using both cubic-anvil large-volume apparatus and laser-heated diamond-anvil cell. *Eos Trans. Am. Geophys. Union* 72(44): 529 (Abstr.)

Litov, E., Anderson, O. L. 1978. The possibility of ferroelectric-like phenomena in the mantle of the Earth. *J. Geophys. Res.* 83: 1692–98

Liu, L.-G. 1974. Silicate perovskite from phase transformations of pyrope-garnet at high pressure and temperature. *Geophys. Res. Lett.* 1: 277–80

Liu, L.-G. 1975. Post-oxide phases of forsterite and enstatite. *Geophys. Res. Lett.* 2: 417–19

Liu, L.-G. 1976. Orthorhombic perovskite phases observed in olivine, pyroxene and garnet at high pressures and temperatures. *Phys. Earth Planet. Inter.* 11: 289–98

Liu, L.-G. 1977. The system enstatite-pyrope at high pressures and temperatures and the mineralogy of the earth's mantle. *Earth Planet. Sci. Lett.* 36: 237–45

Liu, L.-G. 1979. On the 650-km discontinuity. *Earth Planet. Sci. Lett.* 42: 202–8

Liu, L.-G. 1980. Phase relations in the system diopside-jadeite at high pressure and high temperatures. *Earth Planet. Sci. Lett.* 47: 398–402

Liu, L.-G. 1987. New silicate perovskites. *Geophys. Res. Lett.* 14: 1079–82

Liu, L.-G., Bassett, W. A. 1986. *Elements, Oxides, Silicates.* New York: Oxford Univ. Press. 250 pp.

Liu, L.-G., Ringwood, A. E. 1975. Synthesis of a perovskite-type polymorph of $CaSiO_3$. *Earth Planet. Sci. Lett.* 28: 209–11

Liu, X., Wang, Y., Liebermann, R. C., Maniar, P. D., Navrotsky, A. 1991. Phase transition in $CaGeO_3$ perovskite: Evidence from x-ray powder diffraction thermal expansion, and heat capacity. *Phys. Chem. Miner.* In press

Machetel, P., Weber, P. 1991. Intermittent layered convection in a model mantle with an endothermic phase change at 670 km. *Nature* 350: 55–57

Madon, M., Bell, P. M., Mao, H. K., Poirier, J. P. 1980. Transmission electron diffraction and microscopy of synthetic high pressure $MgSiO_3$ phase with perovskite structure. *Geophys. Res. Lett.* 7: 629–32

Madon, M., Guyot, F., Poirier, J. P. 1989. Electron microscopy of high-pressure phases synthesized from natural olivine in diamond anvil cell. *Phys. Chem. Miner.* 16: 320–30

Manghnani, M. H., Syono, Y., eds. 1987. *High Pressure Research in Mineral Physics.* Tokyo: Terra Scientific, Washington, DC: Am. Geophys. Union

Mao, H. K., Chen, L. C., Hemley, R. J., Jephcoat, A. P., Wu, Y., Bassett, W. A. 1989a. Stability and equation of state of $CaSiO_3$ perovskite to 134 GPa. *J. Geophys. Res.* 94: 17,889–94

Mao, H. K., Hemley, R. J., Fei, Y., Shu, J. F., Chen, L. C., et al. 1991. Effect of pressure, temperature, and composition on lattice parameters and density of $(Fe,Mg)SiO_3$-perovskites to 30 GPa. *J. Geophys. Res.* 96: 8069–79

Mao, H. K., Hemley, R. J., Shu, J., Chen, L., Jephcoat, A. P., et al. 1989b. The effect of pressure, temperature, and composition on lattice parameters and density of $(Fe,Mg)SiO_3$-perovskites to 30 GPa. *Annu. Rep. Dir. Geophys. Lab.* 1988–1989: 82–89

Mao, H. K., Yagi, T., Bell, P. M. 1977. Mineralogy of the earth's deep mantle: quenching experiments on mineral compositions at high pressures and temperature. *Carnegie Inst. Washington Yearb.* 76: 502–4

Matsui, M. 1988. Molecular dynamics study

of $MgSiO_3$ perovskite. *Phys. Chem. Miner.* 16: 234–38
Matsui, M., Akaogi, M., Matsumoto, T. 1987. Computational model of the structural and elastic properties of the ilmenite and perovskite phases of $MgSiO_3$. *Phys. Chem. Miner.* 14: 101–6
Matsui, M., Price, G. D. 1991. Simulation of the pre-melting behavior of $MgSiO_3$ perovskite at high pressures and temperatures. *Nature* 351: 735–37
Matsui, Y., Kawamura, K. 1980. Instantaneous structure of an $MgSiO_3$ melt simulated by molecular dynamics. *Nature* 285: 648–49
Matsui, Y., Kawamura, K., Syono, Y. 1982. Molecular dynamics calculations applied to silicate systems: molten and vitreous $MgSiO_3$ and Mg_2SiO_4 under low and high pressures. In *High Pressure Research in Geophysics*, ed. S. Akimoto, M. H. Manghnani, pp. 511–24. Tokyo: Academic
McMillan, P. F. 1989. Raman spectroscopy in mineralogy and geochemistry. *Annu. Rev. Earth Planet. Sci.* 17: 255–83
Meade, C., Jeanloz, R. 1990. The strength of mantle silicates at high pressures and room temperature: implications for the viscosity of the mantle. *Nature* 348: 533–35
Meade, C., Jeanloz, R. 1991. Linear finite strain theory for anisotropic materials. *Eos Trans. Am. Geophys. Union* 72(12): 282 (Abstr.)
Miller, G. H., Stolper, E. M., Ahrens, T. J. 1991a. The equation of state of a molten komatiite. 1. Shock wave compression to 36 GPa. *J. Geophys. Res.* 96: 11,831–48
Miller, G. H., Stolper, E. M., Ahrens, T. J. 1991b. The equation of state of a molten komatiite. 2. Application to komatiite petrogenesis and the hadean mantle. *J. Geophys. Res.* 96: 11,849–64
Miyamoto, M. 1988. Ion migration in $MgSiO_3$-perovskite and olivine by molecular dynamics calculations. *Phys. Chem. Miner.* 15: 601–4
Miyamoto, M., Takeda, H. 1984. An attempt to simulate high pressure structures of Mg-silicates by an energy minimization method. *Am. Mineral.* 69: 711–18
Navrotsky, A., Wiedner, D. J., eds. 1989. *Perovskite: A Structure of Great Interest to Geophysics and Materials Science.* Washington, DC: Am. Geophys. Union. 146 pp.
Navrotsky, A. 1989. Thermochemistry of perovskites. See Navrotsky & Weidner 1989, pp. 67–80
Ohtani, E. 1983. Melting temperature distribution and fractionation in the lower mantle. *Phys. Earth Planet. Inter.* 33: 12–25
Ohtani, E., Kato, T., Ito, E. 1992. Transition metal partitioning between lower mantle and core materials at 27 GPa. *Geophys. Res. Lett.* 18: 85–88
O'Keeffe, M., Bovin, J.-O. 1979. Solid electrolyte behavior of $NaMgF_3$. Geophysical implications. *Science* 206: 599–600
O'Keeffe, M., Hyde, B. G., Bovin, J.-O. 1979. Contribution to the crystal chemistry of orthorhombic perovskites: $MgSiO_3$ and $NaMgF_3$. *Phys. Chem. Miner.* 4: 299–305
O'Neill, B., Brown, D., Jeanloz, R. 1991. Effect of simultaneous Fe and Al substitution on the volume of magnesium-silicate perovskite. *Eos Trans. Am. Geophys. Union* 72(44): 464 (Abstr.)
O'Neill, B., Jeanloz, R. 1990. Experimental petrology of the lower mantle: a natural peridotite taken to 54 GPa. *Geophys. Res. Lett.* 17: 1477–80
Osako, M., Ito, E. 1991. Thermal diffusivity of $MgSiO_3$ perovskite. *Geophys. Res. Lett.* 18: 239–42
Parise, J. B., Wang, Y., Yeganeh-Haeri, A., Cox, D. E., Fei, Y. 1990. Crystal structure and thermal expansion of $(Mg,Fe)SiO_3$ perovskite. *Geophys. Res. Lett.* 17: 2089–92
Peyronneau, J., Poirier, J. P. 1989. Electrical conductivity of the earth's lower mantle. *Nature* 342: 537–39
Pickett, W. E., Cohen, R. E., Krakauer, H. 1991. Lattice instabilities, isotope effect, and high-T_c superconductivity in $La_{2-x}Ba_xCuO_4$. *Phys. Rev. Lett.* 67: 228–31
Poirier, J. P. 1989. Lindemann Law and the melting temperature of perovskites. *Phys. Earth Planet. Inter.* 54: 364–69
Poirier, J. P., Peyronneau, J. 1992. Experimental determination of the electrical conductivity of the material of the Earth's lower mantle. See Syono & Manghnani 1992
Poirier, J. P., Peyronneau, J., Gesland, J. Y., Brebec, G. 1983. Viscosity and conductivity of the lower mantle, an experimental study on a $MgSiO_3$ perovskite analog. *Phys. Earth Planet. Inter.* 32: 273–87
Price, G. D., Wall, A., Parker, S. C. 1989. The properties and behavior of mantle minerals: a computer-simulation approach. *Philos. Trans. R. Soc. London Ser. A* 328: 391–407
Reid, A. F., Ringwood, A. E. 1975. High-pressure modification of $ScAlO_3$ and some geophysical implications. *J. Geophys. Res.* 80: 3363–70
Reynard, B., Price, G. D. 1990. Thermal expansion of mantle minerals at high pressures—a theoretical study. *Geophys. Res. Lett.* 17: 689–92
Richet, P., Mao, H. K., Bell, P. M. 1989.

Bulk moduli of magnesiowüstites from static compression measurements. *J. Geophys. Res.* 94: 3037–45
Ringwood, A. E. 1975. *Composition and Petrology of the Earth's Mantle.* New York: McGraw-Hill. 618 pp.
Ringwood, A. E. 1962. Mineralogical constitution of the deep mantle. *J. Geophys. Res.* 67: 4005–10
Ross, N. L., Hazen, R. M. 1989. Single crystal x-ray diffraction study of $MgSiO_3$ perovskite from 77 to 400 K. *Phys. Chem. Miner.* 16: 415–20
Ross, N. L., Hazen, R. M. 1990. High-pressure crystal chemistry of $MgSiO_3$ perovskite. *Phys. Chem. Miner.* 17: 228–37
Roufosse, M. C., Jeanloz, R. 1983. Thermal conductivity of minerals at high pressure: the effect of phase transitions. *J. Geophys. Res.* 88: 7399–7409
Salje, E. 1989. Characteristics of perovskite-related materials. *Philos. Trans. R. Soc. London Ser. A* 328: 409–16
Sasaki, S., Prewitt, C. T., Lieberman, R. C. 1983. The crystal structure of $CaGeO_3$ and the crystal chemistry of the $GdFeO_3$ type perovskites. *Am. Mineral.* 68: 1189–98
Shearer, P. M. 1990. Seismic imaging of upper-mantle structure with new evidence for a 520-km discontinuity. *Nature* 344: 121–26
Silver, P. G., Carlson, R. W., Olsen, P. 1988. Deep slabs, geochemical heterogeneity, and the large-scale structure of mantle convection: Investigation of an enduring paradox. *Annu. Rev. Earth Planet. Sci.* 16: 477–541
Stixrude, L., Bukowinski, M. S. T. 1990. Fundamental thermodynamic relations and silicate melting with implications for the constitution of *D″*. *J. Geophys. Res.* 95: 19,311–25
Stixrude, L., Bukowinski, M. S. T. 1992. Stability of $(Mg,Fe)SiO_3$ perovskite and the structure of the lowermost mantle. *Geophys. Res. Lett.* In review
Suzuki, I. 1975. Thermal expansion of periclase and olivine, and their anharmonic properties. *J. Phys. Earth* 23: 145–59
Syono, Y., Manghnani, M. H., eds. 1992. *High Pressure Research in Mineral Physics: Applications to Earth and Planetary Sciences.* Tokyo: Terra Scientific. In press
Takahashi, E., Ito, E. 1987. Mineralogy of mantle peridotite along a model geotherm up to 700 km depth. See Manghnani & Syono 1987, pp. 427–37
Tamai, H., Yagi, T. 1989. High-pressure and high-temperature phase relations in $CaSiO_3$ and $CaMgSi_2O_6$ and elasticity of perovskite-type $CaSiO_3$. *Phys. Earth Planet. Inter.* 54: 370–77
Tarrida, M., Richet, P. 1989. Equation of state of $CaSiO_3$ perovskite to 96 GPa. *Geophys. Res. Lett.* 16: 1351–54
Walker, D., Agee, C. 1989. Partitioning "equilibrium," temperature gradients, and constraints on Earth differentiation. *Earth Planet. Sci. Lett.* 96: 49–60
Wall, A., Price, G. D. 1989. Electrical conductivity of the lower mantle: a molecular dynamics simulation of $MgSiO_3$ perovskite. *Phys. Earth Planet. Inter.* 58: 192–204
Wall, A., Price, G. D., Parker, S. C. 1986. A computer simulation of the structure and elastic properties of $MgSiO_3$ perovskite. *Mineral Mag.* 50: 693–707
Wang, Y., Guyot, F., Liebermann, R. C. 1992. Electron microscopic evidence of structural phase transitions in $Mg_{1-x}Fe_xSiO_3$ perovskite and implications for the lower mantle. *J. Geophys. Res.* In press
Wang, Y., Guyot, F., Yeganeh-Haeri, A., Liebermann, R. C. 1990. Twinning in $MgSiO_3$ perovskite. *Science* 248: 468–71
Wang, Y., Weidner, D. J., Liebermann, R. C., Liu, X., Ko, J., et al. 1991a. Phase transition and thermal expansion of $MgSiO_3$ perovskite. *Science* 251: 410–13
Wang, Y., Zhao, Y., Weidner, D. J., Liebermann, R. C., Parise, J. B., Cox, D. E. 1991b. High temperature behavior of $(Mg,Fe)SiO_3$ perovskite at 1 bar. *Eos Trans. Am. Geophys. Union* 72(44): 464 (Abstr.)
Weidner, D. J., Wang, Y., Liebermann, R. C., Vaughan, M. T., Leinenweber, K., et al. 1991. More on high-pressure, high-temperature equation of state of $MgSiO_3$ perovskite. *Eos Trans. Am. Geophys. Union* 72(44): 435 (Abstr.)
Weng, K., Mao, H. K., Bell, P. M. 1982. Lattice parameters of the perovskite phases in the system $MgSiO_3$-$CaSiO_3$-Al_2O_3. *Carnegie Inst. Washington Yearb.* 81: 273–77
Weng, K., Xu, J., Mao, H. K., Bell, P. M. 1983. Preliminary Fourier-transform infrared spectral data on the SiO_6^{8-} octahedral group in silicate-perovskite. *Carnegie Inst. Washington Yearb.* 82: 355–56
Williams, Q. 1990. Molten $(Mg_{0.88}Fe_{0.12})_2SiO_4$ at lower mantle conditions: melting products and structure of quenched glasses. *Geophys. Res. Lett.* 17: 635–38
Williams, Q., Jeanloz, R., McMillan, P. 1987. Vibrational spectrum of $MgSiO_3$ perovskite: zero-pressure Raman and mid-infrared spectra to 27 GPa. *J. Geophys. Res.* 92: 8116–28
Williams, Q., Knittle, E., Jeanloz, R. 1989. Geophysical and crystal chemical sig-

nificance of $(Mg,Fe)SiO_3$ perovskite. See Navrotsky & Weidner 1989, pp. 1–12

Wolf, G., Bukowinski, M. 1985. Ab initio structural and thermoelastic properties of orthorhombic $MgSiO_3$ perovskite. *Geophys. Res. Lett.* 12: 809–12

Wolf, G., Bukowinski, M. S. T. 1987. Theoretical study of the structural and thermodynamic properties of $MgSiO_3$ and $CaSiO_3$ perovskites: implication for lower mantle composition. See Manghnani & Syono 1987, pp. 313–31

Wolf, G. H., Durben, D. J., McMillan, P. F. 1990. Raman spectroscopic study of the vibrational properties and reversion of $CaGeO_3$ and $MgSiO_3$ perovskites as a function of temperature. *Eos Trans. Am. Geophys. Union* 71: 1667 (Abstr.)

Wolf, G. H., Jeanloz, R. 1985. Lattice dynamics and structural distortions of $CaSiO_3$ and $MgSiO_3$ perovskites. *Geophys. Res. Lett.* 12: 413–16

Wood, B. J. 1989. Mineralogical phase change at the 670-km discontinuity. *Nature* 341: 278

Wood, B. J. 1990. Postspinel transformations and the width of the 670-km discontinuity: A comment on "Postspinel transformations in the system Mg_2SiO_4-Fe_2SiO_4 and some geophysical implications" by E. Ito and E. Takahashi. *J. Geophys. Res.* 95: 12681–85

Wood, B. J., Nell, J. 1991. High-temperature electrical conductivity of the lower mantle phase (Mg,Fe)O. *Nature* 351: 309–11

Wright, K., Price, G. D. 1989. Computer simulation of iron in magnesium silicate perovskite. *Geophys. Res. Lett.* 16: 1399–1402

Yagi, T., Bell, P. M., Mao, H. K. 1979c. Phase relations in the system MgO-FeO-SiO_2 between 150 and 700 kbar at 1000°C. *Carnegie Inst. Washington Yearb.* 78: 614–16

Yagi, T., Kusanaga, S., Tsuchida, Y., Fukai, Y. 1989. Isothermal compression and stability of perovskite-type $CaSiO_3$. *Proc. Jpn. Acad. Ser. B* 65: 129–32

Yagi, T., Mao, H. K., Bell, P. M. 1977. Crystal structure of $MgSiO_3$ perovskite. *Carnegie Inst. Washington Yearb.* 76: 516–19

Yagi, T., Mao, H. K., Bell, P. M. 1978a. Structure and crystal chemistry of perovskite-type $MgSiO_3$. *Phys. Chem. Miner.* 3: 97–110

Yagi, T., Mao, H. K., Bell, P. M. 1978b. Effect of iron on the stability and unit-cell parameters of ferromagnesian silicate perovskite. *Carnegie Inst. Washington Yearb.* 77: 837–41

Yagi, T., Mao, H. K., Bell, P. M. 1979a. Lattice parameters and specific volume for the perovskite phase of orthopyroxene composition, $(Mg,Fe)SiO_3$. *Carnegie Inst. Washington Yearb.* 78: 612–13

Yagi, T., Mao, H. K., Bell, P. M. 1979b. Hydrostatic compression of $MgSiO_3$ of perovskite structure. *Carnegie Inst. Washington Yearb.* 78: 613–14

Yagi, T., Mao, H. K., Bell, P. M. 1982. Hydrostatic compression perovskite-type $MgSiO_3$. In *Advances in Physical Geochemistry*, Vol. 2, ed. S. K. Saxena, pp. 317–25. New York: Springer-Verlag

Yeganeh-Haeri, A., Weidner, D. J., Ito, E. 1989a. Elasticity of $MgSiO_3$ in the perovskite structure. *Science* 248: 787–89

Yeganeh-Haeri, A., Weidner, D. J., Ito, E. 1989b. Single crystal elastic moduli of magnesium metasilicate perovskite. See Navrotsky & Weidner 1989, pp. 13–25